DMD Fast Forward. Published on March 20, 2017 as DOI: 10.1124/dmd.116.073932
This article has not been copyedited and formatted. The final version may differ from this version.

TITLE

Prediction of the Transporter-Mediated Drug-Drug Interaction Potential of Dabrafenib and Its Major Circulating Metabolites

Harma Ellens, Marta Johnson, Sarah K. Lawrence, Cory Watson, Liangfu Chen, and Lauren E. Richards-Peterson

Drug Metabolism and Pharmacokinetics, GlaxoSmithKline, King of Prussia, PA 19406

Downloaded from dmd.aspetjournals.org at ASPET Journals on March 30, 2017

DMD Fast Forward. Published on March 20, 2017 as DOI: 10.1124/dmd.116.073932
This article has not been copyedited and formatted. The final version may differ from this version.

RUNNING TITLE: Risk for transporter-mediated drug-drug interactions for dabrafenib and metabolites

* To whom correspondence should be addressed.

Harma M. Ellens, PhD

GlaxoSmithKline, Drug Metabolism and Pharmacokinetics

709 Swedeland Road

King of Prussia, PA 19406

Phone: (610) 416 5741

FAX: 610 270-5041

Email: harmaellens@gmail.com

Number of words in the Abstract: 244

Number of words in the Introduction: 984

Number of words in the Discussion: 1453

Number of text pages: 40

Number of tables: 6

Number of figures: 5

Number of references: 34

Downloaded from dmd.aspetjournals.org at ASPET Journals on March 30, 2017

DMD Fast Forward. Published on March 20, 2017 as DOI: 10.1124/dmd.116.073932
This article has not been copyedited and formatted. The final version may differ from this version.

Abbreviations: A→B, Apical to basolateral; B→A, Basolateral to apical; B→A/A→B ratio, $P_{app\ B\rightarrow A}/P_{app\ A\rightarrow B}$; BCRP, breast cancer resistance protein; CHO, Chinese hamster ovary cell line; DDI, drug-drug interaction; DMEM, Dulbecco's Modified Eagle Medium; DMF, dimethyl formamide; DMSO, dimethyl sulphoxide; DPBS, Dulbecco's Phosphate Buffered Saline; ITC, International Transporter Consortium; K_m, affinity constant; MDCK = Madin Darby canine kidney cells; MDR1, multi-drug resistance protein 1; OATP, organic anion transporting polypeptide; OAT, organic anion transporter; OCT, organic cation transporter; P-gp, P-glycoprotein; P_{app}, apparent permeability; V_{max}, maximum uptake rate.

Downloaded from dmd.aspetjournals.org at ASPET Journals on March 30, 2017

DMD Fast Forward. Published on March 20, 2017 as DOI: 10.1124/dmd.116.073932
This article has not been copyedited and formatted. The final version may differ from this version.

ABSTRACT

The BRAF inhibitor dabrafenib was recently approved for the treatment of certain BRAF V600 mutation-positive tumors, either alone or in combination therapy with the MEK inhibitor trametinib. This article presents the dabrafenib transporter-mediated drug-drug interaction risk assessment, which is currently an important part of drug development, regulatory submission and drug registration. Dabrafenib and its major circulating metabolites (hydroxy-, carboxy- and desmethyl-dabrafenib) were investigated as inhibitors of the clinically relevant transporters Pgp, BCRP, OATP1B1, OATP1B3, OCT2, OAT1 and OAT3. The DDI Guidance risk assessment decision criteria for inhibition of BCRP, OATP1B1 and OAT3 were slightly exceeded and therefore a minor DDI effect resulting from inhibition of these transporters remained possible. Biliary secretion is the major excretion pathway of dabrafenib-related material (71.1% of orally administered radiolabeled dose recovered in feces), while urinary excretion was observed as well (22.7% of the dose). In vitro uptake into human hepatocytes of the dabrafenib metabolites, but not of dabrafenib parent compound, was mediated, at least in part, by hepatic uptake transporters. The transporters responsible for uptake of the pharmacologically active hydroxy- and desmethyl dabrafenib could not be identified, whereas carboxy-dabrafenib was a substrate of several OATPs. Dabrafenib, hydroxy- and desmethyl dabrafenib were substrates of P-gp and BCRP, while carboxy-dabrafenib was not. While a small increase in exposure to carboxy-dabrafenib upon inhibition of OATPs and an increase in exposure to desmethyl-dabrafenib upon inhibition of P-gp or BCRP cannot be excluded, the clinical significance of such increases is likely to be low.

Downloaded from dmd.aspetjournals.org at ASPET Journals on March 30, 2017

DMD Fast Forward. Published on March 20, 2017 as DOI: 10.1124/dmd.116.073932
This article has not been copyedited and formatted. The final version may differ from this version.

INTRODUCTION

The RAS/RAF/MEK/ERK pathway is a critical proliferative pathway in many human cancers (Roberts and Der, 2007). Recently, advances have been made in the development of therapies that specifically target mutated proteins in these cell signaling pathways (Flaherty and McArthur, 2010; Eggermont and Robert, 2011; Heakal et al., 2011; Falchook et al., 2012). BRAF is one of three genes encoding RAF-serine/ threonine kinases. Mutations in BRAF result in a constitutively active kinase that has at least ten times higher activity compared to wild type (Davies et al., 2002). The potent and specific BRAF inhibitors vemurafenib and dabrafenib have significantly improved response rates and overall survival in patients with metastatic melanoma with BRAF V600E or V600K mutations (Ugurel et al., 2016). Dabrafenib was approved in the US as a monotherapy for the treatment of BRAF V600E mutation-positive tumors in 2013 (Hauschild et al., 2012) and as combination therapy with the MEK inhibitor trametinib for the treatment of BRAF V600E or V600K mutation positive tumors in 2014 (Menzies and Long, 2014; Dossett et al., 2015). The combination of dabrafenib and trametinib resulted in a significant delay in the onset of resistance compared to vemurafenib, with a longer median progression free survival, as well as a decreased incidence of skin adverse events (especially skin tumors) associated with administration of BRAF V600E or V600K inhibitors (Robert et al., 2015).

Dabrafenib is highly absorbed, with an oral bioavailability of 95% (Denton et al., 2013). In the human radiolabel study, elimination was mainly via oxidative metabolism, with an estimated 72% of the administered radiolabeled dose eliminated as metabolites, (49.3% in the feces and 22.7% in the urine) and 21.8% of the dose as parent in the feces (biliary

Downloaded from dmd.aspetjournals.org at ASPET Journals on March 30, 2017

secretion and unabsorbed material), with no parent detected in the urine (Bershas et al., 2013). The main metabolites found in excreta and in circulation were hydroxy-dabrafenib, carboxy-dabrafenib and desmethyl-dabrafenib. Averages of 4.52, 9.48 and 14.4% of the administered dose of [^{14}C]dabrafenib were recovered in the feces, and averages of 1.36, 7.11 and 2.13% were recovered in the urine, as hydroxy-, carboxy-, and desmethyl dabrafenib, respectively (Supplementary Table, (Bershas et al., 2013)). The remainder of the radioactivity in these two matrices, besides unchanged parent, was largely in the form of further oxidative metabolites of desmethyl-dabrafenib, plus a glucuronide of hydroxy-dabrafenib (only in urine).

Carboxy-dabrafenib exposure (AUC) at steady state is about eleven fold higher than that of dabrafenib, while hydroxy-dabrafenib and desmethyl-dabrafenib exposures are significant as well, at 90% and 70% of that of dabrafenib (Study BRF113683). Hydroxy-dabrafenib and desmethyl-dabrafenib are potent inhibitors of BRAF V600E or V600K with in vitro anti-proliferative IC_{50} values that are only 2-5 fold higher than dabrafenib, while that of carboxy-dabrafenib is 17-240 fold higher (data on file). Therefore hydroxy- and desmethyl-dabrafenib are expected to contribute to the pharmacological activity of the parent drug.

The potential interaction of dabrafenib and circulating metabolites with cytochrome P450 enzymes (CYPs) was assessed recently (Lawrence et al., 2014). Dabrafenib is metabolized by CYP2C8 and CYP3A4 to hydroxy-dabrafenib, which in turn is metabolized by CYP3A4 to carboxy-dabrafenib. A victim DDI risk was identified for dabrafenib as a substrate of CYP2C8 and/or CYP3A4. Clinical DDI studies showed a 1.47 fold increase in dabrafenib exposure (AUC) upon co-administration with the

Downloaded from dmd.aspetjournals.org at ASPET Journals on March 30, 2017

DMD Fast Forward. Published on March 20, 2017 as DOI: 10.1124/dmd.116.073932
This article has not been copyedited and formatted. The final version may differ from this version.

CYP2C8 inhibitor gemfibrozil and 1.71 fold increase on co-administration with the CYP3A4 inhibitor ketoconazole (Suttle AB, 2014). The risk of dabrafenib and metabolites affecting the pharmacokinetics of sensitive substrates of CYP2C8, 2C9 and 2C19 through CYP inhibition was minor, however, a significant risk was highlighted as a consequence of dabrafenib's PXR and CAR-mediated induction potential. Co-administration of dabrafenib with the CYP3A4 substrate midazolam indeed showed a 74% decrease in midazolam exposure, while co-administration with the CYP2C9 substrate warfarin showed a 37% decrease in exposure of S-warfarin (TAFINLAR, 2016).

The role of drug transporters in drug absorption, distribution and elimination and the potential for pharmacokinetic DDIs through inhibition or induction of drug transporters is now well established. In 2010, the International Transporter Consortium (ITC) published a transporter white paper summarizing key transporters involved in clinically significant DDIs (Giacomini et al., 2010). As concerns about transporter mediated DDIs continue to rise, risk assessments are now an important part of drug development, regulatory submissions and drug registrations (Elsby et al., 2011; Han, 2011; Zhang et al., 2011; Reese et al., 2016). Regulatory DDI guidance documents are available and indicate which transporters should be assessed for this risk during the drug development process (EMA, 2012; FDA, 2012). The studies presented here were conducted to assess the potential of dabrafenib and its major circulating metabolites hydroxy-dabrafenib, carboxy-dabrafenib and desmethyl-dabrafenib to be a perpetrator or a victim of transporter-mediated pharmacokinetic DDIs and provide information for the drug label.

Downloaded from dmd.aspetjournals.org at ASPET Journals on March 30, 2017

DMD Fast Forward. Published on March 20, 2017 as DOI: 10.1124/dmd.116.073932
This article has not been copyedited and formatted. The final version may differ from this version.

The criteria listed in the decision trees in the FDA or EMA DDI guidances were slightly exceeded for inhibition of BCRP, OATP1B1 and OAT3. A drug-drug interaction study evaluating the effect of dabrafenib on rosuvastatin, a BCRP, OATP1B1 and OAT3 substrate, is currently ongoing. Since clearance of dabrafenib-related material is mainly via biliary secretion, dabrafenib and its metabolites were investigated as in vitro substrates of hepatic uptake and efflux transporters. Dabrafenib, hydroxy-dabrafenib and desmethyl-dabrafenib were substrates of P-gp and BCRP, while carboxy-dabrafenib was not. Dabrafenib was not a substrate of hepatic uptake transporters. The uptake of hydroxy- and desmethyl-dabrafenib into hepatocytes was mediated, in part, by as yet unidentified uptake transporters, but these metabolites were shown not to be substrates of OATP1B1, OATP1B3, OATP2B1 or OCT1. Hepatocyte uptake of carboxy-dabrafenib, on the other hand, was largely mediated by OATPs. The worst case risk for hepatic uptake transporter-mediated victim DDIs for carboxy-dabrafenib was assessed using the static equation developed for transport inhibition (Zamek-Gliszczynski et al., 2009). While a small increase in exposure to carboxy-dabrafenib upon inhibition of OATPs and an increase in exposure to desmethyl-dabrafenib upon inhibition of P-gp or BCRP cannot be excluded, the clinical significance of such increases is likely to be low.

Downloaded from dmd.aspetjournals.org at ASPET Journals on March 30, 2017

DMD Fast Forward. Published on March 20, 2017 as DOI: 10.1124/dmd.116.073932
This article has not been copyedited and formatted. The final version may differ from this version.

MATERIALS AND METHODS

Chemicals and Reagents. GF120918A (elacridar) and amprenavir were supplied by Chemical Development, GlaxoSmithKline (RTP, NC). [^{14}C]cimetidine, (ethanolic solution, specific activity 59.7mCi/mmol) was supplied by Selcia Limited, Essex, UK. [^{3}H]digoxin, (ethanolic solution, specific activity 185 GBq/mmol, 37 MBq/mL) was supplied by Amersham Biosciences UK Ltd. [^{3}H]estradiol 17β-D-glucuronide ([^{3}H]EG, ethanolic solution, specific activity 46.9 Ci/mmol), [^{3}H]Estrone Sulfate ([^{3}H]ES, specific activity 45 Ci/mmol) and Hionic-Fluor were obtained from Perkin Elmer Life and Analytical Sciences (Boston, MA). [^{3}H]p-aminohippuric acid ([^{3}H]PAH, specific activity 40-60 Ci/mmol) was obtained from American Radiolabeled Chemicals, Inc. (St. Louis, MO). Rifamycin SV™, cyclosporine A, ketoconazole, quinidine and benzbromarone were procured from Sigma-Aldrich (St. Louis, MO). Montelukast was purchased from Cayman Chemical Company (Ann Arbor, MI) and rosuvastatin from Sequoia Research (Pangbourne, UK). 6-Carboxyfluorescein (6-CFL) was procured from Invitrogen (Grand Island, NY). Dulbecco's modified Eagle's medium (DMEM) with glutamax, foetal bovine serum (FBS), penicillin/streptomycin, geneticin, L-proline, Hanks Balanced Salt Solution (HBSS) and Eagle′s minimum essential medium (MEM) were obtained from Gibco Life Technologies (Grand Island, NY). InVitroGRO™ hepatocyte media was purchased from BioreclamationIVT (Baltimore, MD). The polarized Madin-Darby canine kidney (MDCKII) cell lines heterologously expressing human BCRP (MDCKII-hBCRP) or P-gP (MDCKII-hMDR1) were obtained from stocks purchased from the Netherlands Cancer Institute. The Chinese Hamster Ovary (CHO) cell line heterologously expressing OATP1B1 (CHO-OATP1B1) was obtained from stocks purchased on license from the University of Zurich. The human embryonic kidney cells (HEK-MSRII) and human

Downloaded from dmd.aspetjournals.org at ASPET Journals on March 30, 2017

DMD Fast Forward. Published on March 20, 2017 as DOI: 10.1124/dmd.116.073932
This article has not been copyedited and formatted. The final version may differ from this version.

OATP1B1, OATP1B3, OATP1A2, OATP2B1, OAT1 and OAT3 BacMam baculovirus transduction reagents were supplied by the Biological Sciences group (BSci), GlaxoSmithKline (Collegeville, PA or Ware, UK). Control S_2 cells and S_2 cells expressing human OAT1 and OAT3 were obtained from Kyorin University School of Medicine, Tokyo, Japan (Kimura et al., 2002). Human Embryonic Kidney 293 (HEK293) control and OCT2 expressing cells were from Sekisui Medical Co., Ltd. Cryopreserved human hepatocytes were purchased from Celsis (Chicago, IL) and HEK293 transiently over-expressing OATP1B1*1a were supplied by Corning® (Corning, NY). Twenty-four well tissue culture plates were from Corning. All other reagents used in these investigations were reagent grade or higher and obtained from standard commercial suppliers.

Cell Preparation and Culture Conditions. Frozen cell stocks were prepared for the following cell lines: MDCKII-hMDR1, MDCKII-hBCRP, CHO-OATP1B1 and HEK-MSRII. Cells were grown to approximately 80% confluency in vented tissue culture flasks (adherent cells) or erlenmeyer culture flasks (suspension cultures). Cells were harvested, centrifuged, resuspended to a density of 1-2 x 10^7 cells/mL and subjected to a controlled-rate freeze cycle. The cryovials were transferred on dry ice to permanent storage in the vapor phase of a liquid nitrogen freezer.

Prior to the experiment, cells were rapidly thawed from frozen stocks at 37°C and transferred to sterile centrifuge tubes containing pre-warmed media and centrifuged. After centrifugation the pellet was suspended in the appropriate media and a small aliquot was removed for determining cell density and viability by Trypan Blue exclusion. Cells were then seeded into 24 well plates at the appropriate cell density and incubated at 37°C

Downloaded from dmd.aspetjournals.org at ASPET Journals on March 30, 2017

DMD Fast Forward. Published on March 20, 2017 as DOI: 10.1124/dmd.116.073932
This article has not been copyedited and formatted. The final version may differ from this version.

with 5% CO_2 in a humidified incubator for a specified amount of time. Specific details for each transporter assay are described below.

MDCKII-hMDR1 or MDCKII-hBCRP cells were washed in DMEM with 10% FBS. After the final centrifugation, cells were seeded at a density of 1.2 to 1.6 x 10^5 cells/well in 24-well transwell plates in DMEM with 10% FBS and incubated for three to four days prior to use.

Cryopreserved human hepatocytes were thawed at 37°C and resuspended in 10 to 40mL of *InVitro*GRO CP plating media by gently inverting the tube several times. Cells were diluted to a density of 0.75 x 10^6 viable cells/mL. 500µL of this cell suspension was added to each well of a 24-well collagen coated plate (Becton Dickinson) to give a final density of 0.375 x 10^6 cells/well. Plates were placed into an incubator for approximately 4 hours to allow cell adherence, prior to the experiment.

CHO-OATP1B1 cells were washed in pre-warmed DMEM with glutamax. After centrifugation, cells were re-suspended in cell culture medium (DMEM, 10% FBS, 0.5% (v/v) 10000 units/mL penicillin G sodium, 10000 µg/mL streptomycin, 0.1% (v/v) L-proline (50 mg/mL) and 0.7% (v/v) Geneticin (50 mg/mL)) and seeded into 24-well non-coated polystyrene plates at a density of 1 x 10^6 cells/well. The cell monolayers were used 2 days post seeding. OATP1B1 expression was induced for at least 24 hours prior to use with 5mM sodium butyrate.

HEK-OATP1B1*1a cells were washed in pre-warmed DMEM with 10% FBS and 1% MEM non-essential amino acid solution and centrifuged. After centrifugation the cells were resuspended to achieve a final cell density of 1 x 10^6 cells/mL. Cells were then seeded into poly-D-lysine coated polystyrene 24-well assay plates at a density of

Downloaded from dmd.aspetjournals.org at ASPET Journals on March 30, 2017

0.35 x 10^6 cells/well. Cells were incubated at 37°C with no humidity for 4 hours. Media was aspirated and cells were re-fed with 400µL DMEM media supplemented with sodium butyrate (final concentration 5mM). Cells were cultured for approximately 24 hours with no humidity prior to use in transport assays.

HEK-MSRII cells were washed and resuspended at a density of 1 x 10^6 cells/mL in pre-warmed DMEM-F12 with 10% FBS containing geneticin (0.4 mg/mL) and sodium butyrate (2 mM). BacMam (Kost et al., 2010) reagent containing cDNA for human OATP1B3, OATP1A2, OATP2B1, OAT1 or OAT3 was added to the cell suspension to give the required multiplicity of infection. Cells were then seeded into poly-D-lysine coated polystyrene 24-well assay plates at a density of 4 x 10^5 cells/well for OATP1B3, OATP1A2, or OATP2B1 and 5 x 10^4cells/well for OAT1 or OAT3. Cells were cultured for approximately 48hrs prior to use in transport assays.

Control S2 cells and S2 cells expressing OAT1 and OAT3 were cultured in 75-cm^2 bottom flasks in RITC80-7 containing 5% FBS, 10 mg/L EGF (epidermal growth factor), 80 units/mL insulin, and 10 g/L transferrin and subjected to passage every 2 to 3 days. The cells were trypsinized with 0.05% trypsin·EDTA, resuspended in culture medium and seeded in 24-well non-collagen coated plates at a density of 2.4 to 4.1×10^5 cells/well 48hrs prior to use in transport assay.

Control HEK293 cell and HEK293 cells expressing OCT2 were cultured in 75-cm^2 bottom flasks in DMEM containing 10% FBS, 1% L-glutamine, and 1% antibiotic-antimycotic (10000 units/mL penicillin G sodium, 10000 µg/mL streptomycin sulfate and 25 µg/mL amphotericin B as Fungizone® in 0.85% saline) and subjected to passage every 3 to 4 days. The cells were washed with 1 mL of PBS and then trypsinized with 0.25%

Downloaded from dmd.aspetjournals.org at ASPET Journals on March 30, 2017

trypsin·EDTA. The cells were seeded in Collagen I-Coated 24-well plates at a density of 2.4 to 2.6 × 10^5 cells/well and incubated for 48hrs prior to use in inhibition studies.

In Vitro Transporter Assays.

Pg-P and BCRP inhibition studies. Inhibition of P-gp-mediated transport of [^{3}H]digoxin (30nM) was assessed by determining [B→A] transport in the absence or presence of increasing concentrations of dabrafenib (range: 0.3 – 100μM), hydroxy-dabrafenib and desmethyl-dabrafenib (range: 0.1 – 100μM) and carboxy-dabrafenib (0.08 – 80μM) over a 90 min incubation period. BCRP-mediated transport of [^{14}C]cimetidine (100nM) was assessed by determining [B→A] transport in the absence or presence of increasing concentrations of dabrafenib (range: 0.3 – 100μM), hydroxy-dabrafenib, carboxy-dabrafenib and desmethyl-dabrafenib (range: 0.6 – 200μM) over a 90 min incubation period. In the incubations with dabrafenib (100μM) and desmethyl-dabrafenib (200μM), the monolayer integrity in both test systems was affected, as indicated by increased permeability of the paracellular permeability marker lucifer yellow to >50nm/s, and therefore these data points were excluded. Incubations were performed in triplicate. Incubation media was prepared for each concentration of test compound, including a no inhibition control (no test compound added) and a complete inhibition control (2μM GF120918), by diluting stock solutions of dabrafenib, hydroxy-dabrafenib, desmethyl-dabrafenib (stocks in DMSO) and carboxy-dabrafenib (stock in HPLC grade water) with transport medium (DMEM, with L-glutamine, 25mM HEPES and pyridoxine-HCL but without phenol red and sodium pyruvate). The MDCKII-hMDR1 or MDCK-hBCRP cell monolayers were pre-incubated for 20 min at 37°C (on a plate shaker at approximately 70 rpm) with control media, media containing test compound, or 2μM GF120918, as

Downloaded from dmd.aspetjournals.org at ASPET Journals on March 30, 2017

appropriate, by filling both apical (0.45 mL) and basolateral (1.3 mL) wells. At the end of the pre-incubation period, media was removed and wells were refilled with fresh incubation media containing test compounds and controls. The basolateral media also contained [^{3}H]digoxin (30nM) or [^{14}C]cimetidine (100nM) as well as lucifer yellow (100 μM). Plates were incubated at 37°C on a plate shaker for 90 min as described above. Upon completion of the incubation, 100μL samples were taken from both apical and basolateral compartments and transferred into 96-well Lumaplates. Plates were dried in a drying cabinet overnight and analyzed for total radioactivity using a Top count NXT ™ microplate scintillation and luminescence counter (Perkin Elmer, Waltham, MA). Lucifer yellow concentration in the apical compartments was determined using a SpectraMax Gemini fluorescence microplate reader at wavelengths of λ_{ex} 430 nm and λ_{em} 538 nm. Apparent passive permeability of Lucifer yellow was calculated as described in the calculations section below.

P-gp and BCRP substrate studies. The MDCKII-hMDR1 or MDCKII-hBCRP cell monolayers were pre-incubated for 20 min (37°C) with transport media (on a plate shaker as described above) in the absence or presence of 2μM GF120918 (Pgp and BCRP inhibitor). Transport of 5μM dabrafenib, hydroxy-dabrafenib, carboxy-dabrafenib or desmethyl-dabrafenib, prepared from stock solutions in DMF and diluted in transport media as described previously, was then assessed in two directions (apical to basolateral [A→B] and basolateral to apical [B→A]) in the absence and presence of 2μM GF120918. Pgp studies were conducted in duplicate while BCRP studies were performed in triplicate. Samples were removed from the apical and basolateral compartments after 90 min incubation and analyzed for test compound concentration by

Downloaded from dmd.aspetjournals.org at ASPET Journals on March 30, 2017

DMD Fast Forward. Published on March 20, 2017 as DOI: 10.1124/dmd.116.073932
This article has not been copyedited and formatted. The final version may differ from this version.

LC/MS/MS. Amprenavir (5µm) and [^{14}C]cimetidine (3µM) were used as positive control substrates for P-gp and BCRP, respectively, to ensure assay functionality. Lucifer yellow permeability was assessed in the same transport direction as the test compounds, as described for the transport inhibition experiments above. Efflux transporter inhibition and substrate experiments were regarded as valid where quality control parameters were within acceptable limits. Acceptable values for the P-gp and BCRP inhibition and substrate assays were: lucifer yellow permeability ≤ 50 nm/sec; digoxin, amprenavir or cimetidine mass balance 80 – 120 %; digoxin or cimetidine B>A transport rate ≥ 1.5 pmoles transported/cm^2/h; digoxin, amprenavir or cimetidine transport rate in the presence of 2 µM GF120918 ≤ 30% of uninhibited rate. A compound was considered a P-gp or BCRP substrate when the efflux ratio was > 2 in the absence of GF120918 and close to 1 in the presence of GF120918.

Organic Anion Transporting Polypeptides 1B1 and 1B3 (OATP) Inhibition Studies. The inhibition of human OATP1B1 or OATP1B3 was determined using CHO-OATP1B1 or HEK-MSRII cells, transduced with BacMam baculovirus containing human OATP1B1 or OATP1B3. Cell monolayers were preincubated in triplicate (37°C) for 15 to 30 min in 1mL transport medium (DPBS) in the absence or presence of increasing concentrations of dabrafenib or its metabolites (range: 0.01- 100µM, respectively) or the positive control inhibitor rifamycin (10 µM). Following removal of preincubation media, cells were incubated at 37°C with the positive control substrate [^{3}H]EG (0.02 µM) in the presence of test compound concentrations as described above. The incubation time was 5 min for CHO-OATP1B1 cells, 3 min for HEK-OATP1B1 cells and 10 min for HEK-OATP1B3 cells. [^{3}H]EG uptake was terminated by rinsing rapidly with cold DPBS prior to cell lysis

Downloaded from dmd.aspetjournals.org at ASPET Journals on March 30, 2017

with 400µL of 1% (v/v) Triton X-100. The IC_{50} values were determined as described in the calculations section below. Dabrafenib, at a concentration of 100µM, decreased cell viability and therefore data from that concentration was excluded. Experiments were regarded as valid where quality control parameters were within acceptable limits. Acceptable values for the OATP1B1 and OATP1B3 assays are: ≥ 3-fold signal to noise (average probe substrate uptake rate in uninhibited control wells/average uptake in rifamycin inhibited wells).

Organic Cation Transporter 2 Inhibition Studies (OCT2). The potential of dabrafenib, hydroxy-dabrafenib, carboxy-dabrafenib and desmethyl-dabrafenib to inhibit human OCT2 was determined in a HEK293 cell line stably expressing OCT2 and in control cells. Cell monolayers were preincubated in triplicate (37°C) for 15 min with 300µL HBSS in the absence or presence of increasing concentrations of test compound (range 0.003 – 50µM) or the positive control inhibitor quinidine (300µM). After pre-incubation, the buffer was replaced with 300µL of HBSS containing the positive control substrate [^{14}C]metformin (10µM) in the absence or presence of increasing concentrations of test compound or quinidine. Each mixture was incubated at 37°C for 2 min. After incubation, each solution was removed and the cells were washed with 1 mL of ice-cold 0.2% BSA-PBS once and 1mL of ice-cold PBS twice. All the PBS was removed and 0.1 mol/L NaOH (0.5mL) was added and mixed by pipetting to lyse the cells. The cell lysate was collected and mixed with 10mL of Hionic-Fluor (PerkinElmer) scintillation fluid and measured by LSC. [^{14}C]metformin cleared volume was calculated as: [uptake amount (dpm/well) / protein amount (mg protein/well) x initial [^{14}C]metformin concentration (dpm/µL)]. The % inhibition at each inhibitor concentration was then calculated by

Downloaded from dmd.aspetjournals.org at ASPET Journals on March 30, 2017

subtracting cleared volume in control cells from cleared volume in OCT2 expressing cells. The IC_{50} values were determined as described in the calculations section below. Acceptable values for the OCT2 inhibition are cleared volume of probe substrate in transporter expressing cells/cleared volume of probe substrate in control cells ≥4.

Organic Anion Transporter Inhibition Studies (OAT1 and OAT3). The potential of dabrafenib, hydroxy-dabrafenib, carboxy-dabrafenib and desmethyl-dabrafenib to inhibit human OAT1 and OAT3 was determined in HEK-MSRII cells transduced with OAT1 or OAT3 using BacMam. Cell monolayers were preincubated in triplicate (37°C) for 15 min in 200µL transport medium in the absence and presence of increasing concentrations of dabrafenib and metabolites (0.027 – 100µM) or control inhibitor, benzbromarone (30µM). Following removal of pre-incubation media, cells were incubated with the probe substrate 6-carboxyfluorescein (6-CFL; 5µM) in the absence or presence of increasing test compound concentrations or benzbromarone for 5 min at 37°C. The incubation was terminated by washing 4x with 1mL of ice-cold PBS and uptake of 6-CFL was determined by measuring fluorescence using a FLUOstar Galaxy (BMG Labtechnologies, Offenburg, Germany) at an excitation wavelength of 485 nm and emission wavelength of 535 nm. The IC_{50} values for OAT1 and OAT3 were calculated as described in the calculations section below. Acceptable values for the OAT1 and OAT3 assays are: (average probe substrate uptake in absence of inhibitor/average probe substrate uptake in presence of benzbromarone) ≥ 5-fold.

Transporter-mediated uptake in hepatocytes. Cryopreserved human hepatocytes were pre-incubated in triplicate at 37°C for 15 to 30 min in 1mL transport medium (DPBS with 1% DMSO or DMF at 37°C) with or without a cocktail of hepatic uptake transporter

Downloaded from dmd.aspetjournals.org at ASPET Journals on March 30, 2017

inhibitors. The compounds selected for the inhibitor cocktail included the OATP1B1 and OATP1B3 inhibitor rifamycin SV (Roberts and Der, 2007), the OATP1B1 and OATP1B3 inhibitor cyclosporine A (Falchook et al., 2012), the OATP2B1 inhibitor montelukast (Shirasaka et al., 2012) and the OCT1 inhibitor quinidine (Umehara et al., 2008) at a final concentration of 10µM each. Uptake of dabrafenib (0.3 and 1.0µM), hydroxy-dabrafenib (0.5 and 1.0µM), carboxy-dabrafenib (1 and 30µM), and desmethyl-dabrafenib (0.3 and 1.0µM) was then determined as a function of time and in the absence and presence of the transporter inhibitor cocktail. Hydroxy-dabrafenib (0.35µM) and desmethyl-dabrafenib (0.06µM) were further assessed as OCT1 substrates in human hepatocytes by incubating in the absence and presence of the OCT1 inhibitor, imipramine (10µM). The low substrate concentrations were chosen based on detection limit of the HPLC/MS/MS assay.

Rosuvastatin (5µM) or [^{14}C]metformin (5µM) were added to separate wells as positive control substrates to demonstrate hepatocyte OATP or OCT1 function, respectively. Rosuvastatin uptake was measured over 5 min in the absence and presence of the inhibitor cocktail, while [^{14}C]metformin uptake was measured over 15 min in the absence and presence of imipramine.

Uptake studies were terminated by rinsing rapidly with cold DPBS prior to cell lysis with water. Cell lysates were extracted by liquid-liquid extraction with ethyl acetate, followed by HPLC/MS/MS analysis to determine dabrafenib, hydroxy-dabrafenib, desmethyl-dabrafenib and rosuvastatin concentrations. For uptake of [^{14}C]metformin, cells were lysed with 1% Triton-X and contents of each well were analysed by LSC.

Downloaded from dmd.aspetjournals.org at ASPET Journals on March 30, 2017

DMD Fast Forward. Published on March 20, 2017 as DOI: 10.1124/dmd.116.073932
This article has not been copyedited and formatted. The final version may differ from this version.

Individually expressed transporter uptake studies (OATP1B1, 1B3, 1A2 and 2B1). Transporter-mediated uptake of hydroxy-dabrafenib (0.3 and 1µM), carboxy-dabrafenib (2µM) and desmethyl-dabrafenib (0.3 and 1µM) was investigated in HEK-OATP1B1, OATP1B3, and OATP1A2 expressing and control cells, while hydroxy-dabrafenib and desmethyl dabrafenib were also investigated in HEK-OATP2B1 expressing and control cells. Triplicate cell monolayers were pre-incubated at 37°C for 15 - 30 min in 1mL transport medium with 1% DMSO (DPBS for OATP1B3, 1A2 and 2B1 or HBSS for OATP1B1) in the absence or presence of transporter inhibitors: 10µM rifamycin (OATP1B1 and 1B3), 10µM ketoconazole (OATP1A2) and 10µM montelukast (OATP2B1). The uptake of each compound or positive control substrate ([^{3}H]EG 0.02 µM for OATP1B1 or OATP1B3 and [^{3}H]ES 0.02 µM for OATP1A2 or OATP2B1) was then determined at 0.5, 1, 1.5, 2, 5, 10, 30 and 60 min in the absence or presence of the inhibitors. At the indicated time points cells were washed rapidly with cold buffer as described above for OATP inhibition studies and lysed with water or 1% Triton-X if wells contained radiolabel Concentration of the test compounds in the cell lysates were determined by HPLC/MS/MS or LSC as described above. Signal to noise ratio, or probe substrate uptake in the absence of inhibitor/probe substrate uptake in the presence of inhibitor, was between 3- and 6-fold in hepatocytes as well as in cells expressing individual transporters.

Determination of kinetic parameters for active transport. Kinetic parameters for active transport of hydroxy-dabrafenib, desmethyl-dabrafenib and carboxy-dabrafenib were determined in cryopreserved human hepatocytes and OATP1B1, OATP1B3 and OATP1A2 cells, where appropriate (Menochet et al., 2012). Hepatocytes were pre-incubated in triplicate at 37°C for 15 to 30 min in 1mL transport medium (DPBS with 1%

Downloaded from dmd.aspetjournals.org at ASPET Journals on March 30, 2017

DMSO or DMF). Uptake of hydroxy-dabrafenib and desmethyl-dabrafenib (range 0.1 - 30µM) was then determined at 0.5, 1, 1.5, 2, 5, 15, 30 and 60 min using multiple concentrations of each compound, while carboxy-dabrafenib (range 1 - 100µM) uptake was determined at 0.5, 1.5, 3, 5, 30, 60, 120 and 180 min using multiple concentrations. Uptake kinetics of carboxy-dabrafenib were also determined in OATP1B1, OATP1B3 and OATP1A2 cells using multiple concentrations and time points (concentration ranges: 1 - 100µM for OATP1B1 and OATP1B3 and 0.5 - 50µM for OATP1A2; timepoints: 0.5, 1.5, 3, 5, 10, 30, 60 and 120 mins for OATP1B1; 0.5, 1, 1.5, 2, 5, 15, 30 and 60 minutes for OATP1B3; and 0.5, 0.75, 1, 1.5, 2, 5, 15 and 30 minutes for OATP1A2). At the indicated time points cells were washed rapidly with cold buffer as described above for OATP uptake studies and lysed with water. Concentrations of test compounds in the cell lysates were determined by HPLC/MS/MS. The kinetic parameters for active transport were determined as described in the calculations section below.

Transporter uptake studies (OAT1 and OAT3). Transporter-mediated uptake of carboxy-dabrafenib and positive control substrates [^{3}H]-PAH (OAT1) and [^{3}H]-ES (OAT3) was investigated using S_2 cells expressing human OAT1 or OAT3 and S2 control cells. The cells were preincubated in triplicate for 15 min at 37°C with 0.3mL of DPBS containing 0.1% DMSO. The uptake of carboxy-dabrafenib (0.5, 1, 10, and 100µM) and [^{3}H]-PAH (1 µM) or [^{3}H]-ES 0.05 µM was then determined at 1, 2 and 5 min in transporter expressing and control cells**.** After incubation the cells were washed three times with 1mL of ice-cold DPBS and lysed in 0.5 mL of purified water. Concentrations of the test compounds in the cell lysates were determined by HPLC/MS/MS or LSC as described above. Acceptable values for the OAT1 and OAT3 assays are: cleared volume of each

Downloaded from dmd.aspetjournals.org at ASPET Journals on March 30, 2017

positive control substance in transporter expressing cells/cleared volume of each positive control substrate in control cells ≥ 4.

Sample Preparation and Analysis. Samples containing dabrafenib, hydroxy-dabrafenib or desmethyl-dabrafenib and the analytical internal standard (50, 75 and 50 ng/mL stable isotopically labeled [$^{2}H_{9}$] dabrafenib, [$^{2}H_{6}{}^{13}C_{2}$] hydroxy-dabrafenib or [$^{2}H_{6}{}^{13}C_{2}$] desmethyl-dabrafenib in 50:50 acetonitrile:water, respectively) were extracted from lysates by liquid-liquid extraction with ethyl acetate, followed by HPLC/MS/MS analysis.

Samples containing carboxy-dabrafenib and the analytical internal standard (12 ng/mL [$^{2}H_{6}{}^{13}C_{2}$]carboxy-dabrafenib) were diluted using a solution of 80:20 ethyl alcohol:water, respectively, followed by HPLC/MS/MS analysis.

Cell lysates containing rosuvastatin and the analytical internal standard (stable isotopically labeled rosuvastatin (25 ng/mL [$^{2}H_{7}{}^{15}N_{2}$]rosuvastatin) in 50:50 acetonitrile:water) were extracted by liquid-liquid extraction with tert-butyl methyl ether, followed by HPLC/MS/MS analysis.

HPLC was performed using a Waters Acquity UPLC™ system. Chromatographic separation of dabrafenib, hydroxy-dabrafenib, desmethyl-dabrafenib and rosuvastatin was obtained by using a gradient of 0.1% formic acid in water:acetonitrile on a Waters Acquity BEH C18 (50 x 2.1 mm, 1.7µM) HPLC column. Chromatographic separation of carboxy-dabrafenib was achieved using a gradient of 0.1% formic acid in water: acetonitrile on a Waters Acquity BEH Phenyl (50 x 2.1 mm, 1.7µM) HPLC column at 55ºC. Samples were analyzed by positive ion turbo ionspray MS/MS with an Applied Biosystems/MDS Sciex API 4000. The calibration range for dabrafenib, hydroxy-

Downloaded from dmd.aspetjournals.org at ASPET Journals on March 30, 2017

DMD Fast Forward. Published on March 20, 2017 as DOI: 10.1124/dmd.116.073932
This article has not been copyedited and formatted. The final version may differ from this version.

dabrafenib, desmethyl-dabrafenib and rosuvastatin was 1 to 500ng/mL and for carboxy-dabrafenib was 0.5 to 1000ng/mL. Typical run times were 1.5 min for dabrafenib, hydroxy-dabrafenib and desmethyl-dabrafenib and 1.1 minutes for carboxy-dabrafenib. Raw data was integrated using Applied Biosystems/MDS Sciex software Analyst v 1.6.1. Analyst v 1.6.1 was used to calculate peak area ratios (a weighted $1/x^2$ linear regression was applied to analyte/internal standard peak area ratios versus analyte concentration data) to construct the calibration curves from which the concentrations of compound in the study samples were determined.

Calculations. Apparent passive permeability (Papp) was calculated using the following equation:

$$P_{app} = (\frac{dC_r}{dt}) * \frac{V_r}{(A * C)} \qquad \text{(Eq. 1)}$$

Where C_r is concentration in the receiver compartment, V_r is the volume of the receiver compartment, A is the surface area of the well (1.13 cm^2 for 12-well Transwell®), C is the compound concentration in the dosing solution.

IC_{50} values (the concentration of inhibitor required for 50% inhibition of the monolayer transport or cellular uptake) were determined using the following equation:

$$y = \frac{Range}{1 + \left(\frac{x}{\mathrm{IC}_{50}}\right)^s} + \text{Background} \qquad \text{(Eq. 2)}$$

Where *y* is the transport or uptake rate as a percentage of the uninhibited control, *Range* is the maximum rate of transport (100%) in the absence of inhibitor, Background is the

Downloaded from dmd.aspetjournals.org at ASPET Journals on March 30, 2017

uninhibitable transport rate as percentage of total rate, *x* is the concentration of inhibitor (μM) and s is the slope factor.

Kinetic parameters for transporter mediated uptake into hepatocytes and cells heterologously expressing various OATPs as well as bidirectional passive diffusion clearance and fu_{cell} were determined according to Menochet et al (2012). The differential equations 3 and 4 show the change in cell and media concentration over time, respectively and were solved in MATLAB version 7.2 using the ODE45 solver.

$$\frac{dS_{cell}}{dt} = \frac{\frac{V_{max} \times S_{med,u}}{K_{m,u} + S_{med,u}} + P_{diff,u} \times S_{med,u} - P_{diff,u} \times S_{cell} \times fu_{cell}}{V_{cell}}$$

(Eq. 3)

$$\frac{dS_{med,u}}{dt} = \frac{-\frac{V_{max} \times S_{med,u}}{K_{m,u} + S_{med,u}} - P_{diff,u} \times S_{med,u} + P_{diff,u} \times S_{cell} \times fu_{cell}}{V_{med}}$$

(Eq. 4)

where: S_{cell}= intracellular concentration; $S_{med,u}$= unbound media concentrations; $K_{m,u}$=unbound affinity constant; V_{max}= the maximum uptake rate; $P_{diff,u}$= the unbound passive diffusion clearance; Fu_{cell}= the unbound intracellular fraction; V_{cell}= intracellular volume (3.9 μL/10^6 cells used for hepatocyte experiments; 2.5 μL/10^6 cells used for OATP1B1 uptake experiments; 2.1 μL/10^6 cells used for OATP1B3 uptake experiments; 2.0 μL/10^6 cells used for OATP1A2 uptake experiments. Information on calculation of cellular volume for HEK293 cells can be found in supplemental material); V_{med}= media volume. The relationship between observed and predicted concentrations with 95% confidence intervals are shown in supplemental material.

Downloaded from dmd.aspetjournals.org at ASPET Journals on March 30, 2017

Quantitative DDI Risk Assessment. The steady-state total C_{max} concentrations at the intended dose of 150 mg (twice daily) were used as surrogates for the concentration of inhibitors [I_1] (Clinical study BRF113683, data on file): 2.8 µM for dabrafenib, 1.9 µM for hydroxy-dabrafenib, 11 µM for carboxy-dabrafenib and 0.69 µM for desmethyl-dabrafenib. The estimated concentration of dabrafenib in the gut [I_2] calculated as the dose of inhibitor in 250mL of water is 1155 µM. However, the maximal in vitro solubility of dabrafenib in simulated intestinal fluid in the fed state is only 13.1 µM.

*Perpetrator DDI risk of dabrafenib and metabolites***.** The potential impact of dabrafenib and its circulating metabolites hydroxy-dabrafenib, carboxy-dabrafenib and desmethyl-dabrafenib on the human efflux transporters, breast cancer resistance protein (BCRP) and P-glycoprotein (P-gp) was determined as described in the FDA DDI guidance (FDA, 2012), such that further clinical evaluation of the risk is not necessary if [I_1] /IC_{50} < 0.1 and [I_2] /IC_{50} < 10. The DDI risk potential was also evaluated using the EMA guidance (EMA, 2012), where no further clinical risk assessment is required for intestinal efflux transporters if the $IC_{50} \geq 0.1$*[maximum soluble concentration] which equals [maximum soluble concentration] /$IC_{50} \leq 10$) and for hepatic and renal efflux transporters if the $IC_{50} \geq 50*I_{u,max}$. The potential impact of dabrafenib and circulating metabolites on the human hepatic uptake transporters, (OATP1B1 and OATP1B3) was predicted using the R value approach ($R=1+(fu \times I_{inlet,max}/IC_{50})$ as described by the FDA guidance, where no further clinical assessment is required if the R-Value < 1.25, as well as the approach defined by the EMA guidance, where no further clinical assessment is needed if the $IC_{50} \geq 25*I_{u,inlet,max}$. $I_{inlet,\ max}$ for dabrafenib was estimated as described in the guidances. The potential impact of dabrafenib and circulating metabolites on the human renal uptake transporters, OAT1 and OAT3 was determined according to the FDA guidance, where no

Downloaded from dmd.aspetjournals.org at ASPET Journals on March 30, 2017

clinical DDI study is required if the unbound I_{max}/ IC_{50} <0.1 and the EMA guidance, such that no further clinical studies are needed if the $IC_{50} \geq 50*I_{u,max}$. The perpetrator risks were expressed as R values according to the equations listed in Table 2 and the risk for the combined inhibition by dabrafenib and metabolites was assessed by comparing the 'total R value' to the R value threshold (Table 2).

Victim DDI risk of dabrafenib metabolites. The risk of a hepatic transporter-mediated victim DDI for dabrafenib metabolites could not be assessed based on metabolite levels in the feces, since carboxy-dabrafenib was shown to undergo decarboxylation to desmethyl dabrafenib in this matrix in preclinical species (Richards-Peterson L, 2014). Therefore, the risk assessment was based on renal blood clearance (CL_r) and hepatic blood clearance (CL_h) of the metabolites. CL_r was calculated from the human radiolabel study (amount excreted in urine/blood AUC). $CL_{int,uptake}$ for hepatic uptake was estimated by scaling up the in vitro hepatocyte uptake clearance (based on average initial uptake rates from 2-3 donors) to a liver weight of 1800 gram (Barter et al., 2007) and 117.5 x 10^6 hepatocytes per gram liver (Barter et al., 2008). Hepatic blood clearance was calculated from the $CL_{int,uptake}$ using the well stirred model (Eq. 5), with liver blood flow (Q) being 97 L/h and values for the fraction unbound in blood ($f_{u,b}$) based on fraction unbound in plasma (fu,p; set to 0.01 in case measured value of fu,p is < 0.01) and blood to plasma ratios from Supplemental Table 1.

$$CL_h = \frac{\mathrm{Q} \times f_{u,b} \times CL_{int,uptake}}{\mathrm{Q} + (f_{u,b} \times CL_{int,uptake})} \quad \text{(Eq. 5)}$$

The maximal fold increase resulting from complete inhibition of transporter-mediated uptake in the liver was calculated according to Eq. 6 (Zamek-Gliszczynski et al., 2009),

Downloaded from dmd.aspetjournals.org at ASPET Journals on March 30, 2017

DMD Fast Forward. Published on March 20, 2017 as DOI: 10.1124/dmd.116.073932
This article has not been copyedited and formatted. The final version may differ from this version.

where f_t is the fraction cleared by hepatic uptake transport (Eq. 7) and V_{max}, K_m and $P_{diff,u}$ pertain to uptake into hepatocytes in vitro.

$$fold\ \Delta = \frac{1}{1-f_t} \quad \text{(Eq. 6)}$$

$$f_t = \left[\frac{CL_h}{CL_r + CL_h}\right] \text{x} \left[\frac{\frac{V_{max}}{K_m}}{\frac{V_{max}}{K_m} + P_{diff,u}}\right] \quad \text{(Eq. 7)}$$

Downloaded from dmd.aspetjournals.org at ASPET Journals on March 30, 2017

DMD Fast Forward. Published on March 20, 2017 as DOI: 10.1124/dmd.116.073932
This article has not been copyedited and formatted. The final version may differ from this version.

RESULTS

In Vitro Transporter Inhibition Studies. Inhibition of transport of [^{3}H]digoxin and [^{14}C]cimetidine by dabrafenib, hydroxy-dabrafenib, carboxy-dabrafenib and desmethyl-dabrafenib was assessed in MDCKII-hMDR1 and MDCKII-hBCRP cell lines, respectively. Dabrafenib and circulating metabolites did not inhibit P-gp mediated digoxin transport at any concentration tested (Table 1). Hydroxy-dabrafenib and desmethyl-dabrafenib inhibited human BCRP-mediated cimetidine transport with IC_{50} values of 82 and 5.4μM, respectively. Dabrafenib and carboxy-dabrafenib showed incomplete inhibition of BCRP at the highest test concentrations, 30 and 200μM, respectively, and therefore an IC_{50} could not be determined (Table 1). The BCRP perpetrator risk for dabrafenib and metabolites is indicated in Table 2.

Inhibition of uptake of the OATP1B1 and OATP1B3 probe substrate [^{3}H]EG by dabrafenib, hydroxy-dabrafenib, carboxy-dabrafenib and desmethyl-dabrafenib was investigated in cells overexpressing human OATP1B1 or OATP1B3. Dabrafenib, hydroxy-dabrafenib, carboxy-dabrafenib and desmethyl-dabrafenib inhibited human OATP1B1 with IC_{50} values of 1.4, 4.3, 18 and 0.83μM, respectively and OATP1B3 with IC_{50} values of 4.7, 23, 20 and 4.3μM, respectively (Table 1). The OATP perpetrator DDI risk was evaluated using the extrapolated R-value approach (FDA, 2012) as well as the approach recommended by the EMA (Table 2).

The inhibition of OAT1 and OAT3 by dabrafenib and its metabolites was investigated using 6-CFL as probe substrate in HEK-MSRII cells transduced with OAT1 or OAT3 BacMam baculovirus. For OAT1, IC_{50} values of 6.9, 29, and 10μM were calculated for dabrafenib, hydroxy-dabrafenib and desmethyl-dabrafenib, respectively. The degree of

Downloaded from dmd.aspetjournals.org at ASPET Journals on March 30, 2017

inhibition by carboxy-dabrafenib, up to 100μM, was insufficient to calculate an IC_{50}. For OAT3, IC_{50} values of 3.4, 7.3, 9.0 and 3.4μM were calculated for dabrafenib, hydroxy-dabrafenib, carboxy-dabrafenib and desmethyl-dabrafenib, respectively (Table 1). The inhibition of OCT2 by dabrafenib and metabolites was determined using [^{14}C]metformin (10μM) as probe substrate. Hydroxy-dabrafenib and carboxy-dabrafenib did not inhibit OCT2 mediated transport of [^{14}C]metformin up to 50μM. Dabrafenib and desmethyl-dabrafenib inhibited OCT2-mediated transport of [^{14}C]metformin with IC_{50} values of 9.3 and 28μM, respectively (Table 1). The potential for dabrafenib and its circulating metabolites to cause a drug-drug interaction through inhibition of the renal transporters OAT1, OAT3 and OCT2 is shown in Table 2

In Vitro Passive Permeability. In order to assess the passive permeability of dabrafenib, hydroxy-dabrafenib, carboxy-dabrafenib and desmethyl-dabrafenib, a single test compound concentration of 5 μM was dosed in the presence of GF120918 (inhibitor of Pgp and BCRP) into the apical compartment of duplicate wells of MDCKII-hMDR1 cell monolayers grown in transwells. Dabrafenib, hydroxy-dabrafenib and desmethyl-dabrafenib demonstrated high permeability with an apparent permeability (P_{app}) of 150, 77 and 370nm/s, respectively (Table 3). Carboxy-dabrafenib exhibited low permeability with a P_{app} of 1.8nm/s (Table 3). Note that in the presence of GF120918 the efflux ratio of dabrafenib and metabolites in MDCKII-hMDR1 cells is approximately 1 (Table 4).

In Vitro Transporter Phenotyping Studies. Dabrafenib, hydroxy-dabrafenib and desmethyl-dabrafenib were P-gp substrates with efflux ratios of 36, 120 and 21, respectively, in MDCKII-hMDR1 cells, while carboxy-dabrafenib, with an efflux ratio of 1.8, was not considered a P-gp substrate. Additionally, dabrafenib, hydroxy-dabrafenib

Downloaded from dmd.aspetjournals.org at ASPET Journals on March 30, 2017

DMD Fast Forward. Published on March 20, 2017 as DOI: 10.1124/dmd.116.073932
This article has not been copyedited and formatted. The final version may differ from this version.

and desmethyl-dabrafenib were substrates of human BCRP, with efflux ratios in MDCKII-hBCRP cells of 3.6, 13 and 6.6, respectively, whereas carboxy-dabrafenib with an efflux ratio of 0.7 was not considered a BCRP substrate (Table 4).

In order to identify the transport processes involved in the *in vitro* hepatic uptake, dabrafenib and its metabolites were incubated with cryopreserved human hepatocytes in the absence and presence of a transporter inhibitor cocktail (OATP and OCT1 inhibitors). Dabrafenib uptake in cryopreserved human hepatocytes was not inhibited by the transporter inhibitor cocktail (Figure 2) which, combined with its high passive permeability, is indicative of passive uptake of dabrafenib into hepatocytes, although, theoretically, active uptake of dabrafenib by a transporter or transport mechanism that is not inhibited by this inhibitor cocktail cannot be formally excluded. Uptake of hydroxy-dabrafenib and desmethyl-dabrafenib into cryopreserved human hepatocytes was partially inhibitable by the inhibitor cocktail (Figures 3 and 5), indicating some involvement of transporters in the hepatic uptake of these metabolites. In contrast, the uptake of carboxy-dabrafenib was strongly inhibited, indicating that hepatic uptake of this metabolite occurs largely via a transporter-mediated process, consistent with its low passive permeability (Figure 4). For Figures 2 through 5, the results for only one substrate concentration are shown since the other concentrations gave very similar results. Kinetic parameters for active uptake of hydroxy-dabrafenib, desmethyl-dabrafenib and carboxy-dabrafenib in cryopreserved hepatocytes (using a single lot of cryopreserved hepatocytes only) were obtained using the mathematical model described in the methods section and are shown in Table 5 (see also Supplemental Tables 1 through 3). Fits of the model to the data and the associated 95% CI are shown in Supplemental Figures 1 through 3 and Supplemental Appendices 1 through 3. Even though the

Downloaded from dmd.aspetjournals.org at ASPET Journals on March 30, 2017

DMD Fast Forward. Published on March 20, 2017 as DOI: 10.1124/dmd.116.073932
This article has not been copyedited and formatted. The final version may differ from this version.

potential for further metabolism of hydroxy-dabrafenib and carboxy-dabrafenib in the hepatocytes exists *in vitro*, good fits to the data suggest that incorporation of a metabolism component is not required, indicating that further metabolism is negligible during the relatively short incubation period.

To determine which transporters were responsible for uptake of hydroxy- and desmethyl-dabrafenib into hepatocytes, these metabolites were subsequently incubated with OATP1B1 and OATP1B3 expressing cells in the absence and presence of 10µM rifamycin (OATP1B1 and OATP1B3 inhibitor). They were also investigated as substrates in OATP1A2 or OATP2B1 expressing cells in the absence and presence of 10µM ketoconazole (OATP1A2 inhibitor) or 10µM montelukast (OATP2B1 inhibitor). Uptake of the metabolites was not inhibited by these inhibitors and therefore, these metabolites are most likely not substrates of OATP1B1, OATP1B3, OATP2B1 or OATP1A2. Uptake of hydroxy- and desmethyl dabrafenib into hepatocytes was also not inhibited by 100µM imipramine, indicating they are likely not substrates of OCT1 either. The caveat here is that we cannot formally exclude the possibility that, even though the various inhibitors inhibit the uptake of the respective probe substrates for each of these transporters, they do not inhibit the uptake of hydroxy- and desmethyl-dabrafenib due to the existence of completely independent binding sites for the respective inhibitors and these two metabolites.

Carboxy-dabrafenib on the other hand was shown to be a substrate of OATP1B1, OATP1B3, and OATP1A2, since uptake in transporter expressing cells was inhibitable by the respective transporter inhibitors. Kinetic parameters were therefore determined and are shown in Table 5 (see also Supplemental Tables 4 through 6). Fits to the data

Downloaded from dmd.aspetjournals.org at ASPET Journals on March 30, 2017

DMD Fast Forward. Published on March 20, 2017 as DOI: 10.1124/dmd.116.073932
This article has not been copyedited and formatted. The final version may differ from this version.

and fit statistics are shown in Supplemental Figures 4 through 6 and Supplemental Appendices 4 through 6.

Since a substantial fraction of carboxy-dabrafenib is eliminated via the kidney this metabolite was also investigated as a substrate of renal OATs. Comparison of the uptake in control S2 cells and S2 cells expressing human OAT1 or OAT3 (Kimura et al., 2002) showed signal to noise ratios (S:N) of up to 4 and 14, respectively, indicating that carboxy-dabrafenib was a substrate of both transporters. Positive control substrate (6-CFL) S:N ratios were 65 and 10 for OAT1 and OAT3, respectively. Kinetic parameters were not determined.

Downloaded from dmd.aspetjournals.org at ASPET Journals on March 30, 2017

DMD Fast Forward. Published on March 20, 2017 as DOI: 10.1124/dmd.116.073932
This article has not been copyedited and formatted. The final version may differ from this version.

DISCUSSION

In the present study, we investigated the potential for dabrafenib and its circulating metabolites to interact with clinically relevant uptake and/or efflux transporters in the intestine, liver and kidney. To assess the perpetrator DDI risk, the *in vitro* inhibition of P-gp, BCRP, OATP1B1, OATP1B3, OAT1, OAT3 and OCT2 was determined (Table 1). Although an IC_{50} value for BCRP inhibition could not be determined, a risk was identified for inhibition of intestinal BCRP according to the criterion listed in the FDA guidance. Dabrafenib inhibited BCRP by 52% at 10µM. Assuming an IC_{50} of 10µM results in an I_2/IC_{50} value of [1155µM /10µM] = 115.5, well above the risk threshold. However, the maximal in vitro solubility of dabrafenib in simulated intestinal fluid in the fed state is only 13.1 µM. Therefore, according to the EMA guidance, there is no risk for intestinal BCRP inhibition since the $IC_{50} \geq 0.1$*[maximum soluble concentration]=0.1*13.1=1.31 µM (Table 2). Given the limited solubility of dabrafenib in simulated intestinal fluid, the risk for inhibition of intestinal BCRP appears low.

Dabrafenib and its metabolites demonstrated a slight risk for inhibition of hepatic or renal BCRP with a total R value according to the FDA guidance of 1.49, above the threshold value of 1.1, while the total R value according to the EMA guidance was 1.006, below the threshold of 1.02 (Table 2). A slight risk for inhibition of OATP1B1 by dabrafenib and its metabolites was identified by the EMA, but not the FDA criteria (Table 2). A very slight risk was also identified for inhibition of OAT3 with the total R value just above the EMA, but below the FDA threshold value (Table 2). A clinical DDI study probing the effect of dabrafenib and metabolites on the BCRP, OATP1B1 and OAT3 substrate rosuvastatin is currently ongoing. However, since rosuvastatin is a substrate of

Downloaded from dmd.aspetjournals.org at ASPET Journals on March 30, 2017

DMD Fast Forward. Published on March 20, 2017 as DOI: 10.1124/dmd.116.073932
This article has not been copyedited and formatted. The final version may differ from this version.

multiple transporters, mechanistic extrapolation of such a clinical study to other substrates of these transporters may be difficult (Elsby et al., 2012).

Dabrafenib, hydroxy-dabrafenib and desmethyl dabrafenib were shown to have high passive permeability and to be substrates of the efflux transporters Pgp and BCRP, while carboxy-dabrafenib, with very low passive permeability, was a substrate of several OATPs and OATs. The oral bioavailability of dabrafenib is 95%, indicative of extensive absorption and low first pass intestinal and hepatic metabolism (Denton et al., 2013). While dabrafenib is a substrate of P-gp and BCRP, these efflux transporters do not limit the extent of dabrafenib absorption, likely resulting from the high passive permeability of this compound. These transporters may however contribute to the suggested prolonged absorption of dabrafenib (flip-flop kinetics) (Denton et al., 2013).

Formation of hydroxy-dabrafenib is mediated by CYP2C8 and CYP3A4 and that of carboxy-dabrafenib by CYP3A4 only. Given the high bioavailability and consequently low first pass metabolic clearance, formation of these metabolites is expected to occur mainly in the liver. Desmethyl-dabrafenib can be formed as a product of non-enzymatic decarboxylation of carboxy-dabrafenib under low pH conditions (≤ pH 5) (Bershas et al., 2013). It is formed in hepatocytes in vitro, possibly in endosomes or lysosomes throughout the body (to the extent this low permeability metabolite can gain access to these membrane-bound compartments), but contribution from cytoplasmic enzymes cannot be ruled out. Pgp and BCRP likely contribute to the biliary excretion of dabrafenib, hydroxy- and desmethyl dabrafenib. A relevant effect of a P-gp or BCRP inhibitor on the clearance of dabrafenib is unlikely as the compound is eliminated predominantly by metabolism. This is indicated by the limited fecal excretion of

Downloaded from dmd.aspetjournals.org at ASPET Journals on March 30, 2017

unchanged dabrafenib (21.8%) and the absence of biliary secretion in rat (Richards-Peterson L, 2014) or mouse. Hydroxy-dabrafenib is eliminated predominantly by further oxidation to carboxy-dabrafenib and seems unlikely to undergo significant efflux, suggested by its low fecal excretion (4.52% of the dose after oral administration, Supplementary Table 1 in (Bershas et al., 2013). Hence, no significant DDI effect of a P-gp or BCRP inhibitor is expected. Desmethyl-dabrafenib may be cleared to a significant extent by P-gp and BCRP-mediated biliary or intestinal secretion, but is also further metabolized to several minor metabolites and renally cleared to a limited extent. A DDI effect of a potent dual P-gp and BCRP inhibitor on the clearance desmethyl-dabrafenib cannot be excluded, but is expected to be limited. Carboxy-dabrafenib is one of the main metabolites in the feces. Given that MRP transporters are known to transport amphiphilic organic anions (Keppler, 2011), biliary secretion of carboxy-dabrafenib may involve MRP2, but this was not further investigated. The basolateral secretion of hydroxy- and desmethyl-dabrafenib from hepatocytes into blood is likely to occur at least in part via passive diffusion. Given its very low passive permeability, secretion of carboxy-dabrafenib into the blood might involve a transporter, possibly of the MRP family (not further investigated).

Even compounds that are largely eliminated via hepatic metabolism and/or biliary excretion, such as dabrafenib, may be susceptible to pharmacokinetic drug interactions through inhibition of hepatic uptake transporters. For example, atorvastatin is almost completely metabolized by CYP3A4. However, pharmacogenetic studies have demonstrated that OATP1B1 plays an important role in hepatic elimination of atorvastatin, by determining the rate of hepatic uptake and therefore influencing the pharmacokinetics of this drug (Maeda et al., 2011; Elsby et al., 2012). Dabrafenib and its

Downloaded from dmd.aspetjournals.org at ASPET Journals on March 30, 2017

major circulating metabolites were therefore investigated as substrates of hepatic uptake transporters.

In line with its high passive permeability, dabrafenib uptake in hepatocytes *in vitro* was not inhibitable by inhibitors of OATPs and OCT1 and therefore did not appear to involve uptake transporters. Both hydroxy- and desmethyl-dabrafenib showed some evidence of a saturable uptake process, in addition to passive permeability. The kinetic parameters for active uptake of these metabolites were determined using a single lot of cryopreserved hepatocytes. The active uptake clearance (Vmax/Km) for hydroxy-dabrafenib (11 μL/min/10^6 cells) was about 2 fold greater than the unbound passive diffusion clearance, while that of desmethyl-dabrafenib (34 μL/min/10^6 cells) was 1.6 fold greater. Further transporter phenotyping studies with individually expressed transporters showed that these metabolites were not substrates of OATP1B1, OATP1B3, OATP1A2, OATP2B1 or OCT1, hence the uptake transporter(s) involved in hepatocyte uptake of these metabolites remain(s) unidentified.

The uptake of carboxy-dabrafenib in hepatocytes was almost completely inhibited by a cocktail of OATP and OCT1 inhibitors. The active uptake clearance was 4.1 μL/min/10^6 cells, 45 fold greater than the unbound passive diffusion clearance (determined in the same single lot of cryopreserved hepatocytes as hydroxy- and desmethyl dabrafenib). Further studies showed that it was indeed a substrate of OATP1B1, OATP1B3 and OATP1A2 over-expressed in HEK cells. This is in line with the structural class of this metabolite and its low passive permeability. Carboxy-dabrafenib was also shown to be a substrate of OAT1 and OAT3. No major change in exposure to carboxy-dabrafenib is expected upon inhibition of OAT1 and/or OAT3 because active renal secretion is only

Downloaded from dmd.aspetjournals.org at ASPET Journals on March 30, 2017

one of several elimination pathways, which also include glomerular filtration, fecal elimination and possibly clearance via extra-hepatic decarboxylation.

Hydroxy-dabrafenib, carboxy-dabrafenib and desmethyl-dabrafenib are eliminated via metabolism as well as renal and biliary secretion. The renal clearance of the metabolites (Xe_{0-t}/AUC_{0-t}) (Table 6) was calculated from the human radiolabel study (Bershas et al., 2013), while the hepatic clearance was estimated by scaling in vitro Clint for hepatocyte uptake to whole liver using a well stirred model (Table 6). The potential worst case magnitude of the increase in exposure upon complete inhibition of hepatic uptake transport for carboxy-dabrafenib was estimated to be 1.9 fold, according to Eq 6 (Zamek-Gliszczynski et al., 2009), taking into account the limiting effects of both renal clearance and passive diffusion into hepatocytes. This is clearly an overestimate since the second term in Eq 7 only considers hepatic uptake and assumes metabolism plus biliary secretion is sufficiently fast to not affect the total hepatic intrinsic clearance significantly, which may not be the case given the Clint value measured in human liver microsomes (<0.009 mL/min/mg microsomal protein, data on file). This risk may be further limited by the potential for extra-hepatic decarboxylation of carboxy-dabrafenib. Since the Clint,uptake for hepatic uptake of hydroxy- and desmethyl-dabrafenib was greater than liver blood flow (Table 6) the effect of transport inhibition is likely low.

In summary, the current work has provided insight into the role of transporters in the disposition of dabrafenib and its major circulating metabolites as well as their possible effects on co-administered transporter substrate drugs. These data indicate a low perpetrator DDI risk for dabrafenib and/or metabolites, which is currently being investigated in a clinical DDI study. No victim DDI risk was identified for dabrafenib.

Downloaded from dmd.aspetjournals.org at ASPET Journals on March 30, 2017

DMD Fast Forward. Published on March 20, 2017 as DOI: 10.1124/dmd.116.073932
This article has not been copyedited and formatted. The final version may differ from this version.

While a small increase in exposure to carboxy- dabrafenib upon inhibition of OATPs and an increase in exposure to desmethyl-dabrafenib upon inhibition of Pgp or BCRP cannot be excluded, the clinical significance of such increases is likely to be low.

Downloaded from dmd.aspetjournals.org at ASPET Journals on March 30, 2017

DMD Fast Forward. Published on March 20, 2017 as DOI: 10.1124/dmd.116.073932
This article has not been copyedited and formatted. The final version may differ from this version.

ACKNOWLEDGEMENTS:

We want to acknowledge Elisabeth Minthorne for generating passive permeability and P-gp substrate data for dabrafenib and metabolites, Valeriu Damian-Iordache for MatLab support. We also thank Maciej Zamek-Gliszczynski for helpful suggestions and Markus Zollinger and Annie St Pierre for helpful suggestions and critical reading of the manuscript.

Downloaded from dmd.aspetjournals.org at ASPET Journals on March 30, 2017

DMD Fast Forward. Published on March 20, 2017 as DOI: 10.1124/dmd.116.073932
This article has not been copyedited and formatted. The final version may differ from this version.

AUTHORSHIP CONTRIBUTIONS

Participated in research design: Ellens, Johnson, Lawrence, Watson, Chen and Richards-Peterson

Conducted experiments: Johnson, Watson

Contributed new reagents or analytic tools: NA

Performed data analysis: Ellens, Johnson, Lawrence

Wrote or contributed to the writing of the manuscript: Ellens, Johnson, Lawrence

Downloaded from dmd.aspetjournals.org at ASPET Journals on March 30, 2017

DMD Fast Forward. Published on March 20, 2017 as DOI: 10.1124/dmd.116.073932
This article has not been copyedited and formatted. The final version may differ from this version.

REFERENCES

Barter ZE, Bayliss MK, Beaune PH, Boobis AR, Carlile DJ, Edwards RJ, Houston JB, Lake BG, Lipscomb JC, Pelkonen OR, Tucker GT, and Rostami-Hodjegan A (2007) Scaling factors for the extrapolation of in vivo metabolic drug clearance from in vitro data: reaching a consensus on values of human microsomal protein and hepatocellularity per gram of liver. *Curr Drug Metab* **8:**33-45.

Barter ZE, Chowdry JE, Harlow JR, Snawder JE, Lipscomb JC, and Rostami-Hodjegan A (2008) Covariation of human microsomal protein per gram of liver with age: absence of influence of operator and sample storage may justify interlaboratory data pooling. *Drug Metab Dispos* **36:**2405-2409.

Bershas DA, Ouellet D, Mamaril-Fishman DB, Nebot N, Carson SW, Blackman SC, Morrison RA, Adams JL, Jurusik KE, Knecht DM, Gorycki PD, and Richards-Peterson LE (2013) Metabolism and disposition of oral dabrafenib in cancer patients: proposed participation of aryl nitrogen in carbon-carbon bond cleavage via decarboxylation following enzymatic oxidation. *Drug Metab Dispos* **41:**2215-2224.

Davies H, Bignell GR, Cox C, Stephens P, Edkins S, Clegg S, Teague J, Woffendin H, Garnett MJ, Bottomley W, Davis N, Dicks E, Ewing R, Floyd Y, Gray K, Hall S, Hawes R, Hughes J, Kosmidou V, Menzies A, Mould C, Parker A, Stevens C, Watt S, Hooper S, Wilson R, Jayatilake H, Gusterson BA, Cooper C, Shipley J, Hargrave D, Pritchard-Jones K, Maitland N, Chenevix-Trench G, Riggins GJ, Bigner DD, Palmieri G, Cossu A, Flanagan A, Nicholson A, Ho JW, Leung SY, Yuen ST, Weber BL, Seigler HF, Darrow TL, Paterson H, Marais R, Marshall CJ,

Downloaded from dmd.aspetjournals.org at ASPET Journals on March 30, 2017

Wooster R, Stratton MR, and Futreal PA (2002) Mutations of the BRAF gene in human cancer. *Nature* **417:**949-954.

Denton CL, Minthorn E, Carson SW, Young GC, Richards-Peterson LE, Botbyl J, Han C, Morrison RA, Blackman SC, and Ouellet D (2013) Concomitant oral and intravenous pharmacokinetics of dabrafenib, a BRAF inhibitor, in patients with BRAF V600 mutation-positive solid tumors. *J Clin Pharmacol* **53:**955-961.

Dossett LA, Kudchadkar RR, and Zager JS (2015) BRAF and MEK inhibition in melanoma. *Expert Opin Drug Saf* **14:**559-570.

Eggermont AM and Robert C (2011) New drugs in melanoma: it's a whole new world. *Eur J Cancer* **47:**2150-2157.

Elsby R, Fox L, Stresser D, Layton M, Butters C, Sharma P, Smith V, and Surry D (2011) In vitro risk assessment of AZD9056 perpetrating a transporter-mediated drug-drug interaction with methotrexate. *Eur J Pharm Sci* **43:**41-49.

Elsby R, Hilgendorf C, and Fenner K (2012) Understanding the critical disposition pathways of statins to assess drug-drug interaction risk during drug development: it's not just about OATP1B1. *Clin Pharmacol Ther* **92:**584-598.

EMA (2012) Guideline on the Investigation of Drug Interactions. http://www.ema.europa.eu/docs/en_GB/document_library/Scientific_guideline/2012/07/WC500129606.pdf

Falchook GS, Long GV, Kurzrock R, Kim KB, Arkenau TH, Brown MP, Hamid O, Infante JR, Millward M, Pavlick AC, O'Day SJ, Blackman SC, Curtis CM, Lebowitz P, Ma B, Ouellet D, and Kefford RF (2012) Dabrafenib in patients with melanoma, untreated brain metastases, and other solid tumours: a phase 1 dose-escalation trial. *Lancet* **379:**1893-1901.

Downloaded from dmd.aspetjournals.org at ASPET Journals on March 30, 2017

FDA (2012) Drug Interaction Studies — Study Design, Data Analysis, Implications for Dosing, and Labeling Recommendations. http://www.fda.gov/downloads/drugs/guidancecomplianceregulatoryinformation/guidances/ucm292362.pdf.

Flaherty KT and McArthur G (2010) BRAF, a target in melanoma: implications for solid tumor drug development. *Cancer* **116:**4902-4913.

Giacomini KM, Huang SM, Tweedie DJ, Benet LZ, Brouwer KL, Chu X, Dahlin A, Evers R, Fischer V, Hillgren KM, Hoffmaster KA, Ishikawa T, Keppler D, Kim RB, Lee CA, Niemi M, Polli JW, Sugiyama Y, Swaan PW, Ware JA, Wright SH, Yee SW, Zamek-Gliszczynski MJ, and Zhang L (2010) Membrane transporters in drug development. *Nat Rev Drug Discov* **9:**215-236.

Han HK (2011) Role of transporters in drug interactions. *Arch Pharm Res* **34:**1865-1877.

Hauschild A, Grob JJ, Demidov LV, Jouary T, Gutzmer R, Millward M, Rutkowski P, Blank CU, Miller WH, Jr., Kaempgen E, Martin-Algarra S, Karaszewska B, Mauch C, Chiarion-Sileni V, Martin AM, Swann S, Haney P, Mirakhur B, Guckert ME, Goodman V, and Chapman PB (2012) Dabrafenib in BRAF-mutated metastatic melanoma: a multicentre, open-label, phase 3 randomised controlled trial. *Lancet* **380:**358-365.

Heakal Y, Kester M, and Savage S (2011) Vemurafenib (PLX4032): an orally available inhibitor of mutated BRAF for the treatment of metastatic melanoma. *Ann Pharmacother* **45:**1399-1405.

Keppler D (2011) Multidrug resistance proteins (MRPs, ABCCs): importance for pathophysiology and drug therapy. *Handb Exp Pharmacol***:**299-323.

Downloaded from dmd.aspetjournals.org at ASPET Journals on March 30, 2017

Kimura H, Takeda M, Narikawa S, Enomoto A, Ichida K, and Endou H (2002) Human organic anion transporters and human organic cation transporters mediate renal transport of prostaglandins. *J Pharmacol Exp Ther* **301:**293-298.

Kost TA, Condreay JP, and Ames RS (2010) Baculovirus gene delivery: a flexible assay development tool. *Curr Gene Ther* **10:**168-173.

Lawrence SK, Nguyen D, Bowen C, Richards-Peterson L, and Skordos KW (2014) The metabolic drug-drug interaction profile of Dabrafenib: in vitro investigations and quantitative extrapolation of the P450-mediated DDI risk. *Drug Metab Dispos* **42:**1180-1190.

Maeda K, Ikeda Y, Fujita T, Yoshida K, Azuma Y, Haruyama Y, Yamane N, Kumagai Y, and Sugiyama Y (2011) Identification of the rate-determining process in the hepatic clearance of atorvastatin in a clinical cassette microdosing study. *Clin Pharmacol Ther* **90:**575-581.

Menochet K, Kenworthy KE, Houston JB, and Galetin A (2012) Simultaneous assessment of uptake and metabolism in rat hepatocytes: a comprehensive mechanistic model. *J Pharmacol Exp Ther* **341:**2-15.

Menzies AM and Long GV (2014) Dabrafenib and trametinib, alone and in combination for BRAF-mutant metastatic melanoma. *Clin Cancer Res* **20:**2035-2043.

Reese MJ, Bowers GD, Humphreys JE, Gould EP, Ford SL, Webster LO, and Polli JW (2016) Drug interaction profile of the HIV integrase inhibitor cabotegravir: assessment from in vitro studies and a clinical investigation with midazolam. *Xenobiotica* **46:**445-456.

Richards-Peterson L WT, Mamaril-Fishman D, Bershas D, Karlinsey M, Schubert E, Castellino S, Ouellet D and Gorycki P (2014) Disposition and metabolism of

Downloaded from dmd.aspetjournals.org at ASPET Journals on March 30, 2017

[^{14}C]dabrafenib, a RAF kinase inhibitor, in mice, rats, dogs and humans. *Abstracts from the 10th International ISSX Meeting, Drug Metabolism Reviews* **45:S1:**313.

Robert C, Karaszewska B, Schachter J, Rutkowski P, Mackiewicz A, Stroiakovski D, Lichinitser M, Dummer R, Grange F, Mortier L, Chiarion-Sileni V, Drucis K, Krajsova I, Hauschild A, Lorigan P, Wolter P, Long GV, Flaherty K, Nathan P, Ribas A, Martin AM, Sun P, Crist W, Legos J, Rubin SD, Little SM, and Schadendorf D (2015) Improved overall survival in melanoma with combined dabrafenib and trametinib. *N Engl J Med* **372:**30-39.

Roberts PJ and Der CJ (2007) Targeting the Raf-MEK-ERK mitogen-activated protein kinase cascade for the treatment of cancer. *Oncogene* **26:**3291-3310.

Shirasaka Y, Mori T, Shichiri M, Nakanishi T, and Tamai I (2012) Functional pleiotropy of organic anion transporting polypeptide OATP2B1 due to multiple binding sites. *Drug Metab Pharmacokinet* **27:**360-364.

Suttle AB R-PL, Ouellet D, Aktan G, Gordon M, LoRusso P, Infante JR, Sharma S, Kendra K, Patel M, Arkenau H-T, Middleton MR, Blackman SC and Carson SW (2014) A study of the effects of inhibition of CYP3A4 by ketoconazole (K) and CYP2C8 by gemfibrozil (G) on the pharmacokinetics of Dabrafenib (D). *Clinical Pharmacology & Therapeutics, Posters from the Presidential Trainee Awards* **95:**S89.

TAFINLAR (2016) Product Label https://www.pharma.us.novartis.com/sites/www.pharma.us.novartis.com/files/tafinlar.pdf.

Downloaded from dmd.aspetjournals.org at ASPET Journals on March 30, 2017

Ugurel S, Rohmel J, Ascierto PA, Flaherty KT, Grob JJ, Hauschild A, Larkin J, Long GV, Lorigan P, McArthur GA, Ribas A, Robert C, Schadendorf D, and Garbe C (2016) Survival of patients with advanced metastatic melanoma: The impact of novel therapies. *Eur J Cancer* **53:**125-134.

Umehara KI, Iwatsubo T, Noguchi K, Usui T, and Kamimura H (2008) Effect of cationic drugs on the transporting activity of human and rat OCT/Oct 1-3 in vitro and implications for drug-drug interactions. *Xenobiotica* **38:**1203-1218.

Zamek-Gliszczynski MJ, Kalvass JC, Pollack GM, and Brouwer KL (2009) Relationship between drug/metabolite exposure and impairment of excretory transport function. *Drug Metab Dispos* **37:**386-390.

Zhang L, Huang SM, and Lesko LJ (2011) Transporter-mediated drug-drug interactions. *Clin Pharmacol Ther* **89:**481-484.

Downloaded from dmd.aspetjournals.org at ASPET Journals on March 30, 2017

DMD Fast Forward. Published on March 20, 2017 as DOI: 10.1124/dmd.116.073932
This article has not been copyedited and formatted. The final version may differ from this version.

FOOTNOTES

This work was sponsored by GlaxoSmithKline Pharmaceuticals Inc. Dabrafenib is an asset of Novartis AG as of March 2, 2015.

Downloaded from dmd.aspetjournals.org at ASPET Journals on March 30, 2017

DMD Fast Forward. Published on March 20, 2017 as DOI: 10.1124/dmd.116.073932
This article has not been copyedited and formatted. The final version may differ from this version.

FIGURE LEGENDS

Figure 1. Metabolic pathways of dabrafenib and its main circulating and excretory metabolites.

Figure 2. Time dependent transport of 0.3 µM dabrafenib in cryopreserved human hepatocytes in the absence (black squares) and presence of inhibitor cocktail (rifampicin SV, cyclosporine A, montelukast and quinidine, at 10 µM each) (open squares).

Figure 3. Time dependent transport of 0.5 µM hydroxy-dabrafenib in cryopreserved human hepatocytes in the absence (black squares) and presence of inhibitor cocktail (rifampicin SV, cyclosporine A, montelukast and quinidine, at 10 µM each) (open squares).

Figure 4. Time dependent transport of 30 µM carboxy-dabrafenib in cryopreserved human hepatocytes in the absence (black squares) and presence of inhibitor cocktail (rifampicin SV, cyclosporine A, montelukast and quinidine, at 10 µM each) (open squares).

Figure 5. Time dependent transport of 0.3 µM desmethyl-dabrafenib in cryopreserved human hepatocytes in the absence (black squares) and presence of inhibitor cocktail

Downloaded from dmd.aspetjournals.org at ASPET Journals on March 30, 2017

DMD Fast Forward. Published on March 20, 2017 as DOI: 10.1124/dmd.116.073932
This article has not been copyedited and formatted. The final version may differ from this version.

(rifampicin SV, cyclosporine A, montelukast and quinidine, at 10 μM each) (open squares).

Downloaded from dmd.aspetjournals.org at ASPET Journals on March 30, 2017

Downloaded from dmd.aspetjournals.org at ASPET Journals on March 30, 2017

TABLES

Table 1. Inhibition of P-gp, BCRP, OATP1B1, OATP1B3, OCT2, OAT1 and OAT3 by dabrafenib and metabolites

Transporter	IC_{50} (μM)				Control Inhibitors	Probe Substrates
	Dabrafenib	Hydroxy-Dabrafenib	Carboxy-Dabrafenib	Desmethyl-Dabrafenib		
P-gp	> 30[a]	>100	>80	>100	2μM GF120918	30nM [^{3}H] Digoxin
BCRP	44% @ 30[a,b]	82	42% @ 200[c]	5.4[d]	2μM GF120918	100nM [^{14}C] Cimetidine
OATP1B1	1.4[e]	4.3	18	0.83	10μM Rifamycin	0.02μM [^{3}H]EG
OATP1B3	4.7[e]	23	20	4.3	10μM Rifamycin	0.02μM [^{3}H]EG
OAT1	6.9	29	65%@100[f]	10	30μM Benzabromarone	5μM 6-CFL
OAT3	3.4	7.3	9.0	3.4	30μM Benzabromarone	5μM 6-CFL
OCT2	9.3	>50[g]	>50[g]	28	300μM Quinidine	10μM [^{14}C]Metformin

[a.] Highest test concentration (100μM) of dabrafenib did not meet the lucifer yellow assay acceptance criteria ($P_{7.4}$>50 nm/s), therefore data point excluded.

[b.] Dabrafenib inhibited human BCRP in vitro by 52 & 44% at concentrations of 10 & 30μM, respectively. The amount of inhibition was not sufficient to calculate an IC_{50} value.

[c.] Carboxy-dabrafenib inhibited human BCRP in vitro by 42% at the highest test concentration of 200μM. The amount of inhibition was not sufficient to calculate an IC_{50} value.

[d.] Highest test concentration (200μM) of desmethyl-dabrafenib did not meet the lucifer yellow assay acceptance criteria ($P_{7.4}$>50 nm/s), therefore data point not included.

[e.] Highest test concentration (100μM) of dabrafenib caused a decrease in cell viability (>20%); therefore, data point was not included.

[f.] Carboxy-dabrafenib inhibited human OAT1 in vitro by 65% at the highest test concentration of 100μM. The amount of inhibition was not sufficient to calculate an IC_{50} value.

[g.] Highest concentration tested of parent and metabolites was 50μM.

EG = estradiol 17β-D-glucuronide.

6-CFL = 6-Carboxyfluorescein.

Downloaded from dmd.aspetjournals.org at ASPET Journals on March 30, 2017

Table 2. DDI risk due to transporter inhibition by dabrafenib and metabolites

			Dabrafenib	Hydroxy-dabrafenib	Carboxy-dabrafenib	Desmethyl-dabrafenib		
		R threshold	**R value**	**R value**	**R value**	**R value**	**Total R value**	**Total R=1+Σ(Ri-1)**
BCRP intestinal	EMA	11	2.3				2.310	R=1+I/IC50; I=soluble dose
	FDA	11	116.5				***116.5***	R=1+I/IC50; I=dose in 250 mL
BCRP hepatic/renal	EMA	1.02	1.003	1.001	1.001	1.0013	1.006	R=1+I/IC50; I=Cmax,p,u
	FDA	1.1	1.284	1.023	1.056	1.1270	***1.490***	R=1+I/IC50; I=Cmax,p
OATP1B1	EMA	1.04	1.084	1.016	1.006	1.0083	***1.114***	R=1+I/IC50; I=Iu,inlet,max,b for dabrafenib, I=Cmax,p,u for metabolites
	FDA	1.25	1.084	1.016	1.006	1.0083	1.114	R=1+I/IC50; I=Iu,inlet,max,b for dabrafenib, I=Cmax,p,u for metabolites
OATP1B3	EMA	1.04	1.025	1.003	1.006	1.0016	1.036	R=1+I/IC50; I=Iu,inlet,max,b for dabrafenib, I=Cmax,p,u for metabolites

Downloaded from dmd.aspetjournals.org at ASPET Journals on March 30, 2017

	FDA	1.25	1.025	1.003	1.006	1.0016	1.036	R=1+I/IC50; I=Iu,inlet,max,b for dabrafenib, I=Cmax,p,u for metabolites
OAT1	EMA	1.02	1.004	1.002	1.004	1.0007	1.011	R=1+I/IC50; I=Cmax,p,u
	FDA	1.1	1.004	1.002	1.004	1.0007	1.011	R=1+I/IC50; I=Cmax,p,u
OAT3	EMA	1.02	1.008	1.010	1.012	1.0020	***1.032***	R=1+I/IC50; I=Cmax,p,u
	FDA	1.1	1.008	1.010	1.012	1.0020	1.032	R=1+I/IC50; I=Cmax,p,u
OCT2	EMA	1.02	1.003			1.0002	1.003	R=1+I/IC50; I=Cmax,p,u
	FDA	1.1	1.003			1.0002	1.003	R=1+I/IC50; I=Cmax,p,u

Parameter values used to calculate R values are shown in Supplementary Table 1

Downloaded from dmd.aspetjournals.org at ASPET Journals on March 30, 2017

Downloaded from dmd.aspetjournals.org at ASPET Journals on March 30, 2017

Table 3. Permeability of dabrafenib and metabolites

Compound	A→B P_{app} (nm/s)	A→B P_{app} (nm/s) + GF120918	Permeability Classification
Dabrafenib	16	150	High
Hydroxy-Dabrafenib	4.2	77	High
Carboxy-Dabrafenib	2.5	1.8	Low
Desmethyl-Dabrafenib	27	370	High

Note that in the presence of GF120918, the efflux ratio of dabrafenib and metabolites is approximately 1 (Table 4).

Permeability Classification:	A-B Papp < 5.0	Low
	50.0 > A-B Papp >5.0	Moderate
	A-B Papp > 50.0	High

Table 4. Dabrafenib and metabolites as substrates of Pgp and BCRP

Compound	PgP Efflux Ratio[a]		BCRP Efflux Ratio[a]		Pgp Substrate	BCRP Substrate
	No Inhibitor	+ GF120918	No Inhibitor	+ GF120918		
Dabrafenib	36	1.0	3.6	1.3	Yes	Yes
Hydroxy-Dabrafenib	120	1.0	13	1.3	Yes	Yes
Carboxy-Dabrafenib	1.8	1.3	0.7	1.1	No	No
Desmethyl-Dabrafenib	21	0.9	6.6	1.3	Yes	Yes

[a.] Efflux ratio equals Papp [B→A]) /Papp [A→B].

A compound is considered a substrate when the efflux ratio is > 2 in the absence of GF120918 and close to 1 in the presence of GF120918.

Downloaded from dmd.aspetjournals.org at ASPET Journals on March 30, 2017

Table 5. Kinetic parameters for active uptake of dabrafenib metabolites by OATPs

	Hydroxy-Dabrafenib			Carboxy-Dabrafenib			Desmethyl-Dabrafenib		
	Km (μM)	**Vmax (pmol/min/10^6 cells)**	**Pdiff,u[a] (μL/min/ 10^6 cells)**	**Km (μM)**	**Vmax (pmol/min/ 10^6 cells)**	**Pdiff,u[a] (μL/min/ 10^6 cells)**	**Km (μM)**	**Vmax (pmol/min/ 10^6 cells)**	**Pdiff,u[a] (μL/min/ 10^6 cells)**
Hepatocytes	0.99 ± 0.26	11 ± 2.5	5.1	2.3 ± 0.40	9.4 ± 0.89	0.092	1.8 ± 0.56	62 ± 19	21
OATP1B1		Not a substrate		15 ± 3.1	48 ± 10	0.19		Not a substrate	
OATP1B3		Not a substrate		3.0 ± 0.96	12 ± 2.6	0.42		Not a substrate	
OATP1A2		Not a substrate		2.0 ± 1.5	0.88 ± 0.46	0.28		Not a substrate	

[a.] Pdiff,u = unbound passive diffusion clearance

Downloaded from dmd.aspetjournals.org at ASPET Journals on March 30, 2017

Table 6. Assessment of worst case DDI risk for carboxy-dabrafenib due to inhibition of hepatic uptake transport

	Renal Blood Clearance[a] (mL/h)	In vitro hepatocyte uptake clearance[b] (µL/min/10^6 cells)	In vitro hepatocyte uptake clearance[c] (µL/min/10^6 cells)	Hepatic Clint,uptake[d] (L/h)	Hepatic Blood Clearance[e] (mL/h)	Worst case increase in exposure upon complete inhibition of hepatic uptake transport[f]
Hydroxy-dabrafenib	468	16.2	9.2 (7.7, 10.6)	116	NC[g]	
Carboxy-dabrafenib	390	4.2	1.4 (1.7, 0.6, 2.1)	18	362	1.9
Desmethyl-dabrafenib	2160	55.4	18.8 (27.7, 10.0)	239	NC[g]	

a. Amount excreted in urine/AUC(blood) from the human radiolabel study (Bershas et al., 2013).

b. Based on single determination of Km, Vmax and Pdiff,u.

c. Calculated from initial uptake rates at concentrations at or below the relevant Km indicated in Table 5. Numbers in parentheses are values for individual donors.

d. $CL_{int,uptake}$ was determined by scaling in vitro uptake clearance calculated based on initial uptake rates ([c]) to whole liver assuming liver weight of 1800 gram and 117.5 x 10^6 hepatocytes per gram liver (Barter et al., 2007; Barter et al., 2008).

e. $CL_h = Q_h$ x fu,b x $Cli_{nt,uptake}/Q_h$ + fu,b x $Cl_{int'uptake}$

f. Maximal fold increase equal 1/1-ft (Zamek-Gliszczynski et al., 2009). Calculated based on fractional liver clearance (liver clearance/total clearance) and in vitro hepatocyte ft (active uptake clearance/total uptake clearance).

g. NC: not calculated.

Downloaded from dmd.aspetjournals.org at ASPET Journals on March 30, 2017

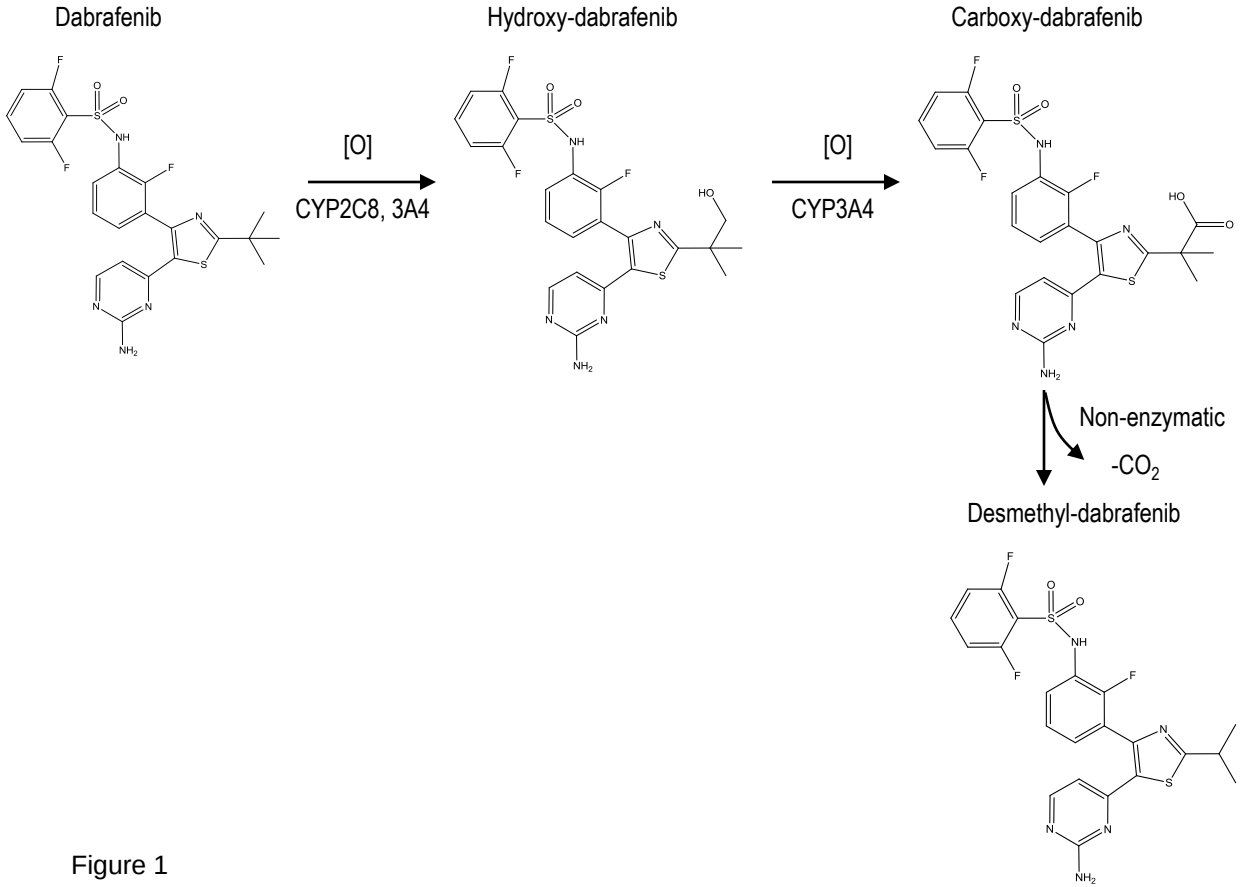

Figure 1

Downloaded from dmd.aspetjournals.org at ASPET Journals on March 30, 2017

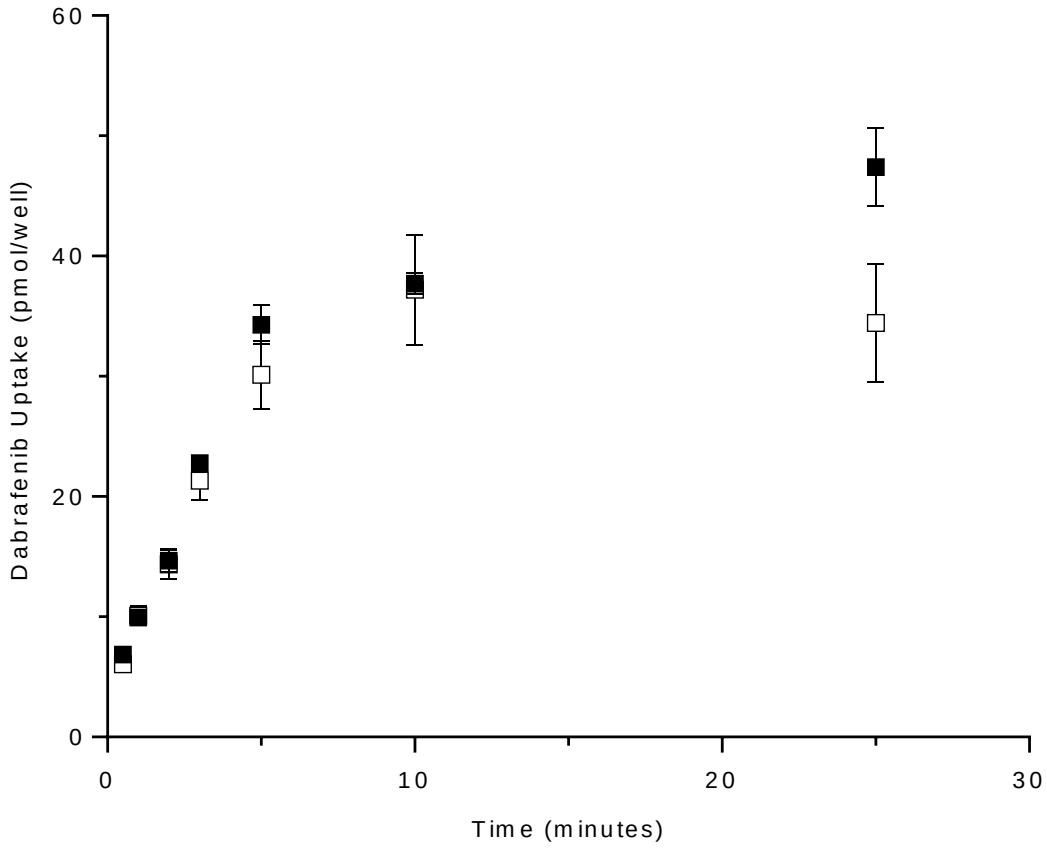

Figure 2

Downloaded from dmd.aspetjournals.org at ASPET Journals on March 30, 2017

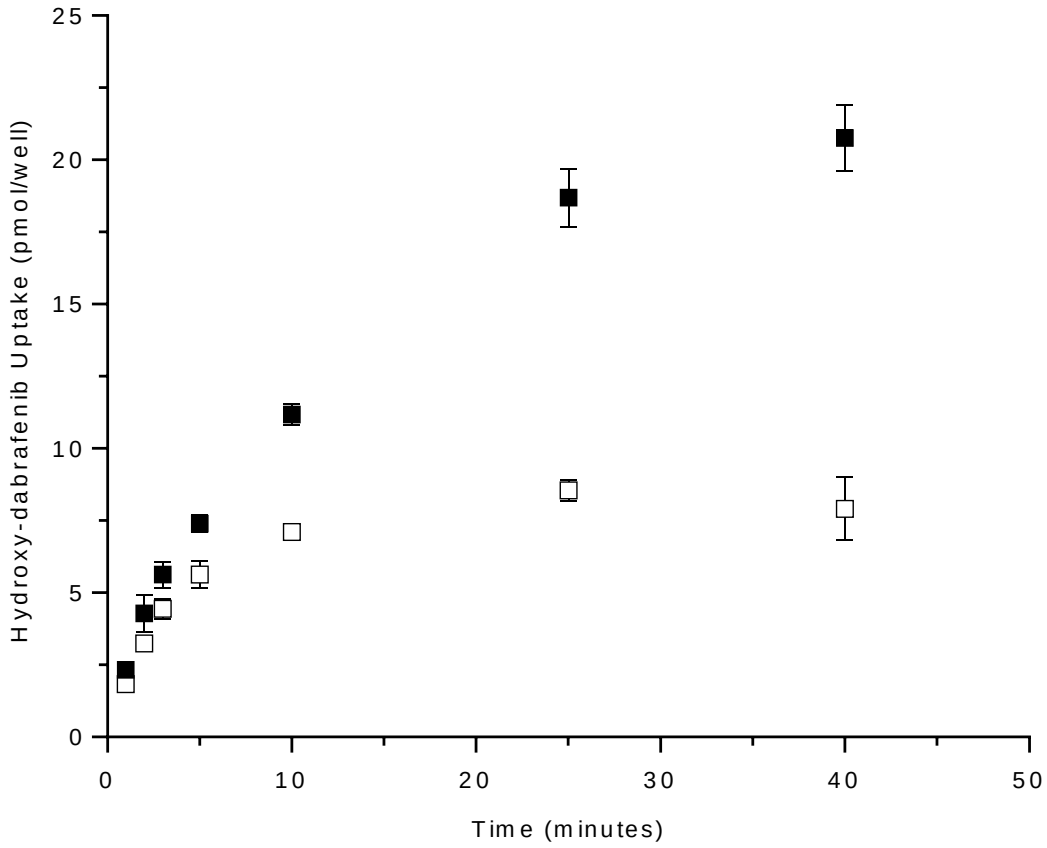

Figure 3

Downloaded from dmd.aspetjournals.org at ASPET Journals on March 30, 2017

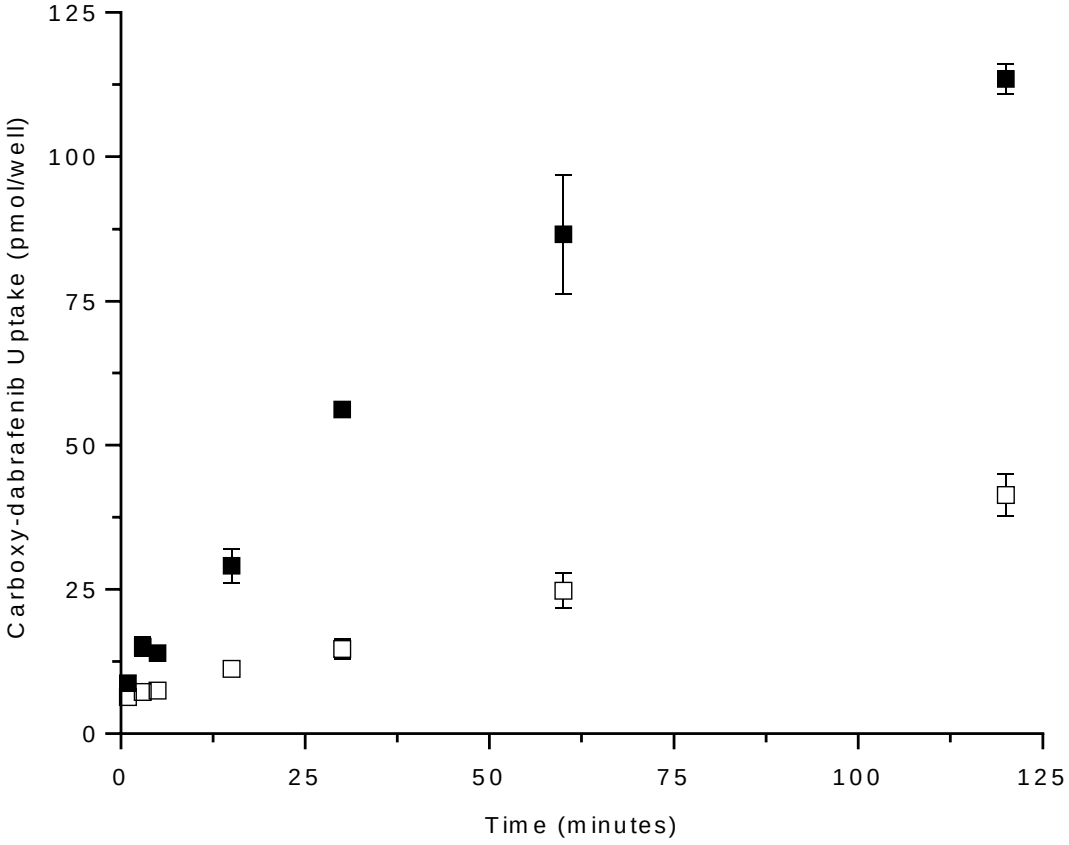

Figure 4

Downloaded from dmd.aspetjournals.org at ASPET Journals on March 30, 2017

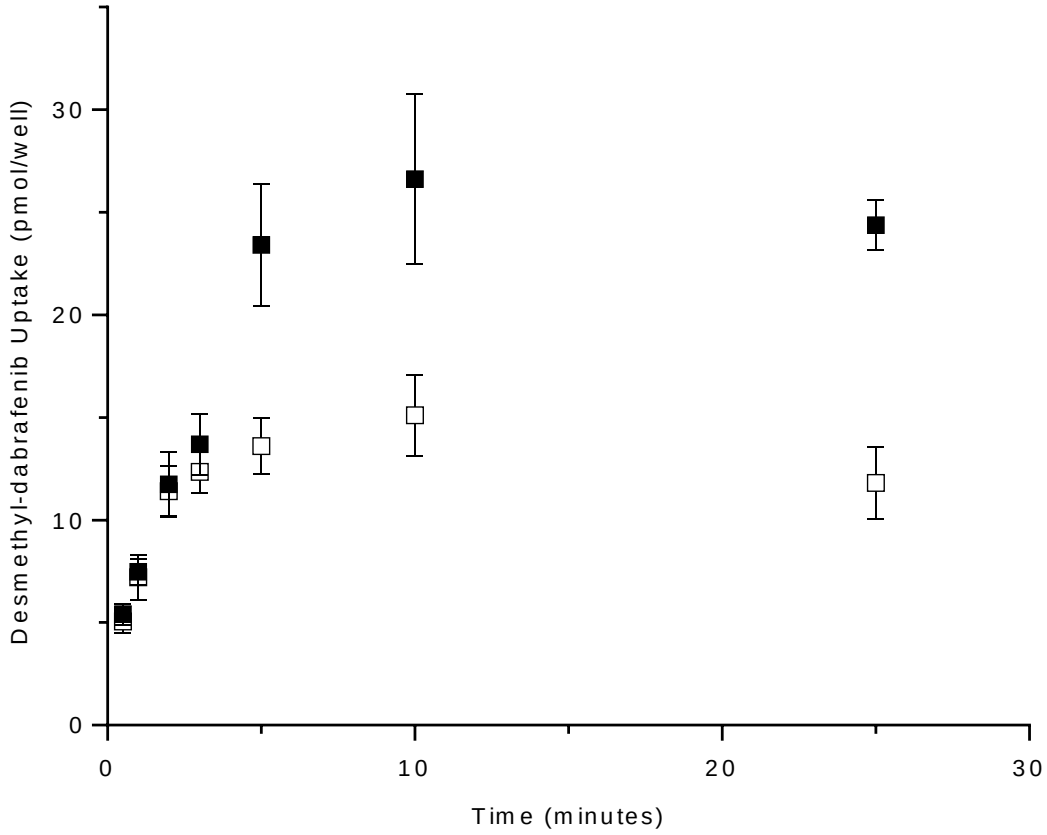

Figure 5

Downloaded from dmd.aspetjournals.org at ASPET Journals on March 30, 2017